INVERSE DESIGN AND BOUNDARY CONTROLLABILITY FOR THE CHROMATOGRAPHY SYSTEM

Giuseppe Maria M Coclite, Carlotta Donadello, Nicola de Nitti, Florian Peru

INVERSE DESIGN AND BOUNDARY CONTROLLABILITY FOR THE CHROMATOGRAPHY SYSTEM

GIUSEPPE MARIA COCLITE, NICOLA DE NITTI, CARLOTTA DONADELLO, AND FLORIAN PERU

Abstract. We consider the prototypical example of the 2×2 liquid chromatography system and characterize the set of initial data leading to a given attainable profile at $t = T$. For profiles that are not attainable at time T, we study a non-smooth optimization problem: recovering the initial data that lead as close as possible to the target in the L^2-norm. We then study the system on a bounded domain and use a boundary control to steer its dynamics to a given trajectory. Finally, we implement a suitable finite volumes scheme to illustrate these results and show its numerical convergence. Minor modifications of our arguments apply to the Keyfitz–Kranzer system.

1. Introduction

The aim of this paper is to generalize some of the recent results in [14, 25, 26] on the backward reconstruction and inverse design for scalar conservation laws in one space dimension,

$$\partial_t u + \partial_x f(u) = 0, \qquad t > 0,\ x \in \mathbb{R}, \tag{1.1}$$

where the flux is strictly convex, to a special class of triangular systems, including the system of multi-component chromatography. In the basic case where only two components are present, the system is given by

$$\begin{cases} \partial_t u_1 + \partial_x \left(\dfrac{u_1}{1+u_1+u_2} \right) = 0, & t > 0,\ x \in \mathbb{R}, \\ \partial_t u_2 + \partial_x \left(\dfrac{u_2}{1+u_1+u_2} \right) = 0, & t > 0,\ x \in \mathbb{R}, \\ u_1(0,x) = \bar{u}_1(x), & x \in \mathbb{R}, \\ u_2(0,x) = \bar{u}_2(x), & x \in \mathbb{R}, \end{cases} \tag{1.2}$$

where $u_1, u_2 \in \mathbb{R}_+$ are the components' concentrations. The interested reader can refer to [4, 5] for a complete well-posedness analysis of this system that also applies in several space dimensions. However, as we limit our attention to the one-dimensional setting, we strongly rely on the approach and the results in [27], which we also recall briefly in Section 2.1. The results in [10], established in the more general setting of Temple class systems, show that, for any initial condition in $L^\infty(\mathbb{R})$, the Cauchy problem for (1.2) admits a unique entropy admissible solution. In particular, the system admits a continuous semi-group of solutions[1]

$$\begin{array}{rccc} S^+ : & \mathbb{R}_+ \times L^\infty(\mathbb{R};\mathbb{R}^2) & \to & L^1_{\mathrm{loc}}(\mathbb{R};\mathbb{R}^2) \\ & (t, U_0 = (\bar{u}_1, \bar{u}_2)) & \mapsto & S^+_t\,(U_0)\,. \end{array} \tag{1.3}$$

The inverse design problem consists of the following steps:

(1) for any given $T > 0$, characterize the set of profiles $U_T = (u_1^T, u_2^T) \in L^\infty(\mathbb{R};\mathbb{R}^2)$ for which there exists at least one initial condition $(\bar{u}_1, \bar{u}_2) \in L^\infty(\mathbb{R};\mathbb{R}^2)$ such that $S^+_T(\bar{u}_1, \bar{u}_2) = (u_1^T, u_2^T)$;
(2) for each of such attainable profiles, characterize the set of initial data leading to them, $\mathfrak{I}(U_T)$;

2020 *Mathematics Subject Classification.* 35L65.

Key words and phrases. Hyperbolic systems of conservation laws; triangular systems; 2×2 chromatography system; entropy solutions; renormalized solutions; inverse design; boundary controllability.

[1]The system is not strictly hyperbolic, therefore the semi-group is not Lipschitz continuous (see [12, Section 7]).

(3) for profiles that cannot be attained by a trajectory of the system, recover the initial data leading to their "best possible approximation";
(4) find the element (or the elements) of $\mathfrak{I}(U_T)$ that is optimal for the desired application in the sense that it minimizes a suitable cost functional.

Of course, developing suitable numerical schemes is also relevant to compare the evolution of different solutions and investigate the set of possible initial conditions.

In the case of scalar conservation laws with strictly convex flux, (1.1), the set of states in $L^\infty(\mathbb{R})$ attainable by Kružkov entropy solutions at time $T > 0$ was characterized in [1, 2, 8, 21] as follows:

$$\mathcal{A}_T(\mathbb{R}, f) = \Big\{ u \in L^\infty(\mathbb{R}) : \ \exists \rho : \mathbb{R} \to \mathbb{R}, \text{ right continuous, non-decreasing such that } f'(u) = \frac{x - \rho(x)}{T} \Big\} \tag{1.4}$$

Furthermore, for every $u_T \in \mathcal{A}_T(\mathbb{R}, f)$, there exists a unique *isentropic solution* $u : [0, T] \times \mathbb{R} \to \mathbb{R}$ that verifies $u(T, \cdot) = u_T$. For general conditions toward the existence of isentropic solutions of conservation laws (possibly in several space dimensions), see [23].

The full characterization of the set of inverse designs $\mathcal{I}(u_T)$ corresponding to a reachable target $u_T \in \mathcal{A}_T(\mathbb{R}, f)$ was given in [14, Theorem 4.1] and, by different arguments, in [26, Theorem 1]. Furthermore, in [14, Propositions 5.1 & 5.2], Colombo and Perrollaz studied the topological and geometric properties of $\mathcal{I}(u_T)$. Finally, in [25], Liard and Zuazua computed the distance, with respect to the L^2-norm, between a possibly unattainable target profile and the set of attainable profiles at time T for the Burgers' equation, and proposed an algorithm to construct elements of $\mathcal{I}(u_T)$ containing any fixed number of shock discontinuities.

More recently, in [15], Colombo, Perrollaz, and Sylla generalized the analysis of [14] to scalar conservation laws whose flux may explicitly depend on the x variable (under suitable assumptions).

Some of the essential ingredients in the results above, such as the duality with Hamilton-Jacobi equations and the Lax-Oleinik formula, do not apply to systems; thus, control results in this setting are much less abundant. In [9], the authors characterized the set of attainable profiles at time T for a class of triangular systems, called non-resonant systems, by means of a backward reconstruction procedure relying on the entropies of the systems. For some systems endowed with a particular structure, such as the chromatography system (1.2) and the Keyfitz–Kranzer system (2.19), the backward reconstruction procedure can be performed on the system itself, without exploiting the entropies to write a companion equation. In this setting, it is possible to further the analysis of inverse design, as we do in the present paper (see Section 2.4). Section 2.3 summarizes the main results in [9]. It should be noticed, however, that the set of attainable profiles for genuinely nonlinear hyperbolic systems in the Temple class defined on a bounded domain and driven by boundary controls was first characterized by Ancona and Coclite in [7]. In particular, they showed that the positive waves entering through the boundaries decay in time, so that their density (expressed in terms of Riemann coordinates) is inversely proportional to their distance from their entry point on the boundary.

In addition, in Section 3, we consider a (possibly unattainable) profile and study its projection onto the set of attainable profiles. This extends the results in [25], where an analogous L^2-minimization problem was considered for scalar conservation laws. Moreover, in Section 4, we prove a theorem on the boundary controllability to trajectories of (1.2) similar to the result of [17]. Finally, in Section 5, we describe the implementation and prove the numerical convergence of a finite volume scheme inspired from the one in [9] and the results in [25], which we used to produce all the examples throughout the paper.

2. Preliminaries

2.1. **Well-posedness of the Chromatography system.**

Using the change of variables

$$v := u_1 + u_2 \quad \text{and} \quad w := u_1 - u_2,$$

the system (1.2) reduces to the coupling between a scalar conservation law and a linear continuity equation:

$$\begin{cases} \partial_t v + \partial_x \left(\dfrac{v}{1+v} \right) = 0, & t > 0,\ x \in \mathbb{R}, \\ \partial_t w + \partial_x \left(\dfrac{w}{1+v} \right) = 0, & t > 0,\ x \in \mathbb{R}, \\ v(0,x) = \bar{u}_1(x) + \bar{u}_2(x), & x \in \mathbb{R}, \\ w(0,x) = \bar{u}_1(x) - \bar{u}_2(x), & x \in \mathbb{R}. \end{cases} \tag{2.1}$$

The well-posedness in L^∞ of system (2.1) in one space dimension can be seen as an application of the results in [27], where Panov considered the (more general) problem

$$\begin{cases} \partial_t (A\rho) + \partial_x (B\rho) = 0, & t > 0,\ x \in \mathbb{R}, \\ A(0,x)\rho(0,x) = A(0,x)\rho_0(x), & x \in \mathbb{R}, \end{cases} \tag{2.2}$$

under the assumptions

(1) A and B in $L^\infty(\mathbb{R}_+ \times \mathbb{R})$;
(2) $\partial_t A + \partial_x B = 0$ in $\mathcal{D}'((0,+\infty) \times \mathbb{R})$;
(3) there exists $N : \mathbb{R} \to \mathbb{R}$ such that $\varepsilon N(\varepsilon) \to 0$ as ε tends to zero and for all $\varepsilon > 0$, $|B| \leq N(\varepsilon)(A + \varepsilon)$ a.e. in $(0,+\infty) \times \mathbb{R}$;
(4) $\operatorname{ess\,lim}_{t \to 0^+} A(t,\cdot) = A(0,\cdot)$ in $L^1_{\mathrm{loc}}(\mathbb{R})$ and $A(0,\cdot) \in L^\infty(\mathbb{R})$.

For any given bounded initial condition ρ_0, there exists a bounded function ρ, called *generalized solution* of (2.2), such that, for any test function φ in $C_0^\infty([0,+\infty) \times \mathbb{R})$,

$$\int_0^{+\infty} \int_{\mathbb{R}} \Big((A\rho)\partial_t \varphi + (B\rho)\partial_x \varphi \Big) \,\mathrm{d}x \,\mathrm{d}t + \int_{\mathbb{R}} A(0,x)\rho_0(x)\varphi(0,x) \,\mathrm{d}x = 0. \tag{2.3}$$

Moreover, every generalized solution ρ enjoys the following properties.

Strong traces: The initial condition is satisfied in the sense that in $L^1_{\mathrm{loc}}(\mathbb{R})$

$$\operatorname*{ess\,lim}_{t \to 0^+} A(t,x)\rho(t,x) = A(0,x)\rho_0(x),$$

and for all $T > 0$, there exists $\operatorname*{ess\,lim}_{t \to T^-} A(t,x)\rho(t,x)$ in $L^1_{\mathrm{loc}}(\mathbb{R})$.

Reversibility: If ρ is a generalized solution of problem (2.2) and the identity $A(T,x)\rho(T,x) = A(T,x)\rho_T(x)$ holds in the sense of strong traces, then $t \mapsto \rho(T-t)$ is a generalized solution of

$$\begin{cases} \partial_t (A\rho) - \partial_x (B\rho) = 0, & t > 0,\ x \in \mathbb{R}, \\ A(0,x)\rho(0,x) = A(0,x)\rho_T(x), & x \in \mathbb{R}. \end{cases} \tag{2.4}$$

Uniqueness: If $A(0,x)\rho_0(x) = 0$ a.e. on $\mathbb{R}$ then $A(t,x)\rho(t,x) = 0$ a.e. on $\mathbb{R}_+ \times \mathbb{R}$.

Renormalization: for any function μ in $C(\mathbb{R})$ the function $\mu \circ \rho$ satisfies

$$\begin{cases} \partial_t \left(A(\mu(\rho)) \right) + \partial_x \left(B(\mu(\rho)) \right) = 0, & t > 0,\ x \in \mathbb{R}, \\ \left(\mu(\rho) \right)(0,x) = \mu\left(\rho_0(x) \right), & x \in \mathbb{R}, \end{cases} \tag{2.5}$$

in the sense of (2.3).

In the case of system (2.1), the scalar equation

$$\partial_t v + \partial_x \left(\frac{v}{1+v} \right) = 0, \qquad t > 0,\ x \in \mathbb{R}, \tag{2.6}$$

admits a unique entropy solution in $L^\infty(\mathbb{R}_+ \times \mathbb{R})$ starting from any initial condition $v_0 \in L^\infty(\mathbb{R})$. This allows us to define the divergence-free vector field $t \mapsto (A(t,x), B(t,x))$, for $A(t,x) = v(t,x)$ and $B(t,x) = \dfrac{v(t,x)}{1+v(t,x)}$, satisfying all of the hypothesis above.

Owing to the strict concavity of the flux, the solution's profiles $v(t,\cdot)$ are of bounded variation at any $t>0$, which also ensures the existence of traces along time-like curves (e.g., the sides boundaries of the domain if we work in $(0,T)\times[0,L]$, as in Section 4), and are in $C(\mathbb{R}_+;L^1_{\mathrm{loc}}(\mathbb{R}))$, so that we also have strong traces at $t=0$ and $t=T$. Then Panov's theorem guarantees that, for any given $z_0\in L^\infty(\mathbb{R})$, there exists a unique generalized solution in $L^\infty(\mathbb{R}_+\times\mathbb{R})$ of

$$\begin{cases}\partial_t(vz)+\partial_x\left(\dfrac{vz}{1+v}\right)=0, & t>0,\ x\in\mathbb{R},\\ z(0,x)=z_0(x), & x\in\mathbb{R}.\end{cases}\tag{2.7}$$

From this, we can recover the solution for the chromatography system in the form (2.1) and (1.2):

- the solution w of the transport equation appearing in (2.1) can be seen as $w=vz$ if we set $z_0=(\bar u_1-\bar u_2)/v_0$;
- the solution (u_1,u_2) of (1.2) can be seen as $(u_1=vz_1,u_2=vz_2)$ if z_i (for $i\in\{1,2\}$) is the solution of (2.7) corresponding to the initial condition $z_{0,i}=\bar u_i/v_0$.

In both cases, since the z satisfies the maximum principle and we consider $v_0=\bar u_1+\bar u_2$ with $\bar u_i\ge 0$, we have that $\|z\|_{L^\infty(\mathbb{R})}\le 1$.

To summarize, we are referring to the concept of solution introduced in the following definition, which was initially proposed in connection with the Keyfitz–Kranzer system (see [18, 28]).

Definition 2.1 (Solution of the chromatography system in the form (1.2))**.** *Let $\bar U=(\bar u_1,\bar u_2)\in L^\infty(\mathbb{R};\mathbb{R}^2)$ be the initial conditions imposed to the system* (1.2)*. A function $U=(u_1,u_2)\in L^\infty((0,T)\times\mathbb{R};\mathbb{R}^2)$ is a* strong generalized entropy solution *for the system* (1.2) *if $U=\left(\dfrac{v+w}{2},\dfrac{v-w}{2}\right)$, where*

- *the function v is the Kružkov entropy solution of*

$$\begin{cases}\partial_t v+\partial_x\left(\dfrac{v}{1+v}\right)=0, & t\in(0,T),\ x\in\mathbb{R},\\ v(0,x)=\bar u_1(x)+\bar u_2(x), & x\in\mathbb{R}\,;\end{cases}\tag{2.8}$$

- *the function w is given by $w=vz$, where z is the solution of* (2.7) *in the weak sense with initial datum $z_0(x)=\dfrac{\bar u_1(x)-\bar u_2(x)}{\bar u_1(x)-\bar u_2(x)}$ and coefficients $A=v$ and $B=\dfrac{v}{1+v}$.*

In the above definition, the value of $\dfrac{\bar u_1(x)-\bar u_2(x)}{\bar u_1(x)-\bar u_2(x)}$ can be taken arbitrary ±1 at points where $\bar U=0$.

Owing to the renormalization property, the definition above is equivalent to the definition of *renormalized entropy solution* used in [5], which we write here for completeness.

Definition 2.2 (Renormalized entropy solution of the chromatography system in the form (1.2))**.** *The function $U\in L^\infty((0,T)\times\mathbb{R};\mathbb{R}^2)$ is a renormalized entropy solution for the system* (2.1) *if*

- *the function v is the Kružkov entropy solution of* (2.8)*;*
- *the function w is given by $w=zv$ where, for any test function $\varphi\in C_0^\infty([0,T)\times\mathbb{R})$ and any continuous function μ, z satisfies*

$$\int_0^T\int_{\mathbb{R}}\left(v\mu(z)\partial_t\varphi+\frac{1}{1+v}\mu(w)\partial_x\varphi\right)\mathrm{d}x\,\mathrm{d}t+\int_{\mathbb{R}}v(0,x)\mu(z_0(x))\varphi(0,x)\,\mathrm{d}x=0.$$

By direct computations (see also [9]), the entropy/entropy-flux pairs for the systems (2.1) take the following form:

$$\mathcal{E}(v,w):=\eta(v)+v\mu\left(\frac{w}{v}\right),\tag{2.9}$$

$$\mathcal{Q}(v,w):=q(v)+\frac{v}{1+v}\mu\left(\frac{w}{v}\right),\tag{2.10}$$

where η is any entropy function for (2.8) and $\mu\in C(\mathbb{R})$. Therefore, the strong generalized entropy solutions coincide with the entropy solutions for the system.

2.2. **Backward semigroups.** In what follows, we shall denote $\mathfrak{S}_t^+(V_0)$ the (forward) semigroup associated with the system (2.1), $\mathcal{S}_t^+(v_0)$ the (forward) Kružkov semigroup associated with the scalar conservation law in (2.1), by $\mathscr{S}_t^+[v](w_0)$ the (forward) semigroup associated to the linear continuity equation (2.1) for a given v. Using the change of variables $(t,x)\mapsto(T-t,-x)$ and (2.4), we also define the backward semigroup $\mathscr{S}_t^-[v](w_T)$. Additionally, we define $\mathcal{S}_t^-(v_T)$ the backward Kružkov semigroup associated with the scalar conservation law in (2.1). The solutions $\mathcal{S}_t^+(v_0)$ and $\mathcal{S}_t^-(v_T)$ are the zero-viscosity limits of the solutions $\mathcal{S}_t^{+,\varepsilon}(v_0)$ and $\mathcal{S}_t^{-,\varepsilon}(v_T)$, defined as follows: $v^{\varepsilon,+}(t,\cdot)=\mathcal{S}_t^{+,\varepsilon}(v_0)$ is the solution of the (forward) viscous conservation law

$$\begin{cases}\partial_t v^{\varepsilon,+}(t,x)+\partial_x f(v^{\varepsilon,+}(t,x))=\varepsilon\partial_{xx}^2 v^{\varepsilon,+}(t,x), & t>0,\ x\in\mathbb{R},\\ v^{\varepsilon,+}(0,x)=v_0(x), & x\in\mathbb{R},\end{cases}\tag{2.11}$$

and $v^{\varepsilon,-}(t,\cdot)=\mathcal{S}_t^{-,\varepsilon}(v_T)$ is the solution of

$$\begin{cases}\partial_t v^{\varepsilon,-}(t,x)+\partial_x f(v^{\varepsilon,-}(t,x))=-\varepsilon\partial_{xx}^2 v^{\varepsilon,-}(t,x), & 0<t<T,\ x\in\mathbb{R},\\ v^{\varepsilon,-}(T,x)=v_T(x), & x\in\mathbb{R}.\end{cases}\tag{2.12}$$

Using the change of variable $(t,x)\mapsto(T-t,-x)$, the backward equation above is well-defined as it coincides with the equation in (2.11). We consider now a convex entropy $\eta\in C^2(\mathbb{R})$ and the corresponding entropy-flux $q\in C^2(\mathbb{R})$ satisfying $\eta'(\xi)=q'(\xi)f'(\xi)$ for all $\xi\in\mathbb{R}$. For any $\varepsilon>0$ and any positive test function $\varphi\in C_c^1((0,T)\times\mathbb{R})$, the solution of (2.12) satisfies the reverse-direction entropy inequality:

$$\int_0^T\int_{\mathbb{R}}\left(\eta(v^{\varepsilon,-})\partial_t\varphi+q(v^{\varepsilon,-})\partial_x\varphi\right)\mathrm{d}x\,\mathrm{d}t\le\varepsilon\int_0^T\int_{\mathbb{R}}\eta(v^{\varepsilon,-})\partial_{xx}^2\varphi\,\mathrm{d}x\,\mathrm{d}t,\tag{2.13}$$

which means that, in the limit $\varepsilon\to0$, the sequence $(v^{\varepsilon,-})_\varepsilon$ converges (in the strong topology of L^1_{loc} and up to a subsequence) to a limit point v^- satisfying

$$\partial_t\eta(v^-)+\partial_x q(v^-)\ge0,\qquad 0<t<T,\ x\in\mathbb{R},\tag{2.14}$$

in the sense of distributions. This condition allows us to characterize the limits of the vanishing viscosity approximation (2.12) and define the semigroup $\mathcal{S}_*^-(v_T)$. Whenever the limit solution $v^-=\mathcal{S}_*^-(v_T)$ is isentropic, i.e. satisfies (2.14) as an equality, it is also the unique limit of the solutions of (2.11) corresponding to the initial condition $x\mapsto v_0(x)=v^-(T,x)=\mathcal{S}_T^-(v_T)(x)$. Therefore, we have $v_T(x)=\mathcal{S}_T^+\left(\mathcal{S}_T^-(v_T)\right)(x)$.

If, on the contrary, the solution v^- strictly produces entropy, in the sense that

$$\partial_t\eta(v^-)+\partial_x q(v^-)>0,\qquad 0<t<T,\ x\in\mathbb{R},$$

holds in the sense of distributions for any convex entropy η, then we can conclude that v^- contains at least one entropy-producing jump discontinuity, i.e. a discontinuity propagating along the time-like curve $t\mapsto(t,s(t))$ which satisfies the Rankine-Hugoniot condition but such that $v^-(t,s(t)^-)>v^-(t,s(t)^+)$. Of course, in this definition, we take into account the fact that the flux function of the nonlinear conservation law in (2.1) is concave.

Whenever the initial condition v_0 of (2.11) contains a jump discontinuity of this kind at $x=\bar{x}$, with $v_0(\bar{x}^-)>v_0(\bar{x}^+)$, the corresponding limit solution v^+ would develop a rarefaction wave centered at $x=\bar{x}$. This means that, for any v_T such that v^- strictly produces entropy, the function $\mathcal{S}_T^+\left(\mathcal{S}_T^-(v_T)\right)$ does not necessarily coincide with v_T. The results on the characterization of attainable profiles at time T for scalar nonlinear conservation laws allow us to say that actually $v_T\neq\mathcal{S}_T^+\left(\mathcal{S}_T^-(v_T)\right)$; indeed, $v_T\in\mathcal{A}_T(\mathbb{R},f)$ if and only if there exists an initial condition from which an isentropic solution of the equation reaches v_T at time T. By Kružkov's uniqueness theorem, such an isentropic solution, whenever it exists, must coincide with v^-.

Remark 2.1 (Characterization of the backward semigroup)**.** *In* [9]*, the authors call backward semigroup for the nonlinear conservation law the operator defined in terms of the forward semigroup as*

follows:

$$\begin{array}{rccc} \mathcal{K}^- : & \mathbb{R}_+ \times (L^\infty(\mathbb{R})) & \to & L^\infty(\mathbb{R}) \\ & (t, v_T) & \mapsto & \mathcal{S}_t^+ \left(v_T(r)\right)(r(x)), \end{array} \tag{2.15}$$

where $r(x) = -x$. If $v_T \in \mathcal{A}(\mathbb{R}, f)$, this gives the isentropic solution reaching the profile v_T at time T. A direct comparison of Riemann problems shows that $\mathcal{K}^-$ and $\mathcal{S}^-$ coincide.

We exploit the characterization above in the definition of our numerical scheme in Section 5.

2.3. **Attainable profiles for triangular systems.** In this section, we summarize the main results in [9]. The authors consider triangular systems of the form

$$\begin{cases} \partial_t u + \partial_x f(u) = 0, & t > 0,\ x \in \mathbb{R}, \\ \partial_t v + \partial_x (g(u) v) = 0, & t > 0,\ x \in \mathbb{R}, \end{cases} \tag{2.16}$$

where the $f : \mathbb{R} \to \mathbb{R}$ and $g : \mathbb{R} \to \mathbb{R}$ satisfy the following assumptions.

(F1) *Regularity of the flux*: $f \in C^2(\mathbb{R})$.
(F2) *Local uniform convexity of the flux*: for all compact sets $K \in \mathbb{R}$, there exists $\alpha_K > 0$ such that $f''_{|_K} \geq \alpha_K$.
(G1) *Regularity of the transport coefficient*: $g \in C^1(\mathbb{R})$.

The main theoretical result applying under the hypothesis above is the following theorem (see [9, Theorems 3.1 and 4.2]).

Theorem 2.1 (Characterization of reachable profiles)**.** *Let us assume that f satisfies (F1)–(F2) and g satisfies (G1). Given $T > 0$, we consider a target state $U_T = (u_T, v_T)$ in $L^\infty(\mathbb{R}; \mathbb{R}^2)$.*

Non attainable states: *The condition $u_T \in \mathcal{A}_T(\mathbb{R}, f)$ is necessary for the target state $U_T = (u_T, v_T)$ being attainable at time t, for any $v_T \in L^\infty(\mathbb{R})$.*

Non resonant case: *If the system additionally satisfies the condition*

(NR) Non-resonance*: $f'(\xi) \neq g(\xi)$ for all $\xi \in \mathbb{R}$,*

then the condition $u_T \in \mathcal{A}_T(\mathbb{R}, f)$ is also sufficient to establish the attainability of U_T at time T for any $v_T \in L^\infty(\mathbb{R})$. More precisely, there exists a unique initial datum $U_0 = (u_0, v_0)$ and a unique isentropic solution $U = (u, v)$ on $(0, T) \times \mathbb{R}$ with $U(0, \cdot) = U_0$ and $U(T, \cdot) = U_T$.

Resonant case: *If the system does not satisfy (NR) and $u_T \in \mathcal{A}_T(\mathbb{R}, f)$, then*

- *for any given $\varepsilon > 0$ there exist an initial datum $U_0^\varepsilon = (u_0^\varepsilon, v_0^\varepsilon)$ and an isentropic solution $U^\varepsilon = (u^\varepsilon, v^\varepsilon)$ on $(0, T) \times \mathbb{R}$ with $U^\varepsilon(0, \cdot) = U_0^\varepsilon$ and $\| U^\varepsilon(T, \cdot) - U_T \|_{L^1_{\mathrm{loc}}(\mathbb{R})} \leq C\varepsilon$;*
- *if u_T belongs to the set $\mathbb{A}_T = W^{1,\infty}(\mathbb{R}) \cap \left(\bigcup_{\delta > 0} \mathcal{A}_{T+\delta}(f, \mathbb{R}) \right)$, which is a dense subset of $\mathcal{A}_T(\mathbb{R}, f)$, then there exists a unique initial datum $U_0 = (u_0, v_0)$ and a unique function $U = (u, v)$ on $(0, T) \times \mathbb{R}$ with $U(0, \cdot) = U_0$ and $U(T, \cdot) = U_T$ such that[2] u is the unique isentropic solution of the first equation of (2.16) such that $u(T, \cdot) = u_T$ and v is the unique DiPerna–Lions renormalized solution (see [16, 3]), of the second equation of (2.16) such that $v(T, \cdot) = v_T$.*

In particular, under the assumptions (F1), (F2), (G1), and (NR), the set of states in $L^\infty(\mathbb{R})$ that are attainable by entropy solutions of system (2.16) is given by

$$\mathfrak{A}_T(\mathbb{R}) = \mathcal{A}_T(\mathbb{R}, f) \times L^\infty(\mathbb{R}). \tag{2.17}$$

As already noticed in [9], the chromatography system in the form (2.1) satisfies all of these conditions. We should stress, however, that a generic element of the set of the attainable profiles for (2.1) at time $T > 0$,

$$\mathfrak{A}_T(\mathbb{R}) = \left\{ (v_T, w_T) \ : \ v \in \mathcal{A}_T \left(\mathbb{R}, v \mapsto \frac{v}{1+v} \right) \text{ and } w \in L^\infty(\mathbb{R}) \right\},$$

[2]When the condition (NR) is violated the systems only admits entropies which are linear with respect to the second component of the solution. Therefore, the uniqueness of entropy solutions is not guaranteed.

does not correspond to an attainable profile for the system (1.2) because it might happen that $((v_T + w_T)(x), (v_T - w_T)(x))$ is not in $\mathbb{R}^2_+$ for almost every $x \in \mathbb{R}$, while all physically relevant solutions of (1.2) are in $L^\infty(\mathbb{R}_+ \times \mathbb{R}; \mathbb{R}^2_+)$. Therefore, we define

$$\mathsf{A}_T(\mathbb{R}) = \left\{ (v_T, w_T) \ : \ \begin{array}{l} v \in \mathcal{A}_T\left(\mathbb{R}, v \mapsto \dfrac{v}{1+v}\right) \text{ and there exists} \\ z \in L^\infty(\mathbb{R}_+ \times \mathbb{R}; [-1,1]) \text{ such that } w_T = z v_T \end{array} \right\}$$

and we say that $U_T = (u_1^T, u_2^T)$ is attainable for system (1.2) if and only if $(v_T := u_1^T + u_2^T, w_T = u_1^T - u_2^T) \in \mathsf{A}_T$.

For completeness and because the analysis in the next sections fully applies to this case, we briefly recall the result in [9] about the Keyfitz–Kranzer system, introduced in [22]:

$$\partial_t U + \partial_x(\phi(|U|)U) = 0, \qquad t > 0, \ x \in \mathbb{R}, \tag{2.18}$$

where $\phi : \mathbb{R}_+ \to \mathbb{R}$ is a smooth function such that $\lim_{r \to 0+} r\phi(r) = 0$ and $U(t,x) \in \mathbb{R}^{m+1}$ (with $m \geq 1$). Introducing the variables (r, n) as $r = |U|$ and $n = U/|U|$, the system (2.18) is formally equivalent to a triangular system endowed with a constraint:

$$\begin{cases} \partial_t r + \partial_x(\phi(r)r) = 0, & t > 0, \ x \in \mathbb{R}, \\ \partial_t(rn) + \partial_x(\phi(r)rn) = 0, & t > 0, \ x \in \mathbb{R}, \\ |n| = 1, & t > 0, \ x \in \mathbb{R}. \end{cases} \tag{2.19}$$

Strong generalized entropy solution for the first two equations of (2.19) associated with the initial conditions $r_0 = |U_0|$ and $n_0 = U_0/|U_0|$ automatically satisfy the constraint $|n| = 1$ a.e. on $\{(t,x) : r(t,x) > 0\}$ as a consequence of the renormalization property; therefore, they correspond to entropy solutions of the system in the form (2.18). We collect the result in the following theorem (see [9, Theorem 3.9]).

Theorem 2.2 (Attainable profiles for the Keyfitz–Kranzer system)**.** *Let us assume that $r \mapsto r\phi(r)$ in system* (2.18) *is strictly convex on $[a,b] \subset [0, +\infty)$. Given $T > 0$, the target datum $U_T \in \mathbb{R}^{m+1}$ is attainable by a unique strong generalized entropy solution for the Keyfitz–Kranzer system* (2.18) *if and only if $r_T = |U_T|$, taking values in the interval $[a,b]$, belongs to the set $\mathcal{A}_T(\mathbb{R}, r \mapsto r\phi(r))$.*

Analogously, the target datum $(r_T, n_T) \in L^\infty(\mathbb{R}_+ \times \mathbb{R}; [a,b] \times \mathbb{S}^{m+1})$ is attainable by a unique strong generalized entropy solution for the Keyfitz–Kranzer system (2.19) *if and only if r_T belongs to the set $\mathcal{A}_T(\mathbb{R}, r \mapsto r\phi(r))$.*

2.4. **Inverse design for the chromatography system.** Given an attainable target state $U_T = (u_1^T, u_2^T)$ we identify the set of possible initial conditions $U_0 = (\bar{u}_1, \bar{u}_2)$ which lead to U_T at time $t = T$ through the following procedure. We first notice that if both components of the target state $U_T = (u_1^T, u_2^T)$ are null functions on an interval $[a,b]$ of positive measure, then all backward characteristics of the equation for v, (2.6), issued from points in $[a,b]$ are classical and have slope 1. This means that all the initial conditions associated with solutions of (2.6) which reach the profile $v_T = u_1^T + u_2^T$ must coincide (and take the value zero) on the interval $[a - T, b - T]$.

Wherever v_T is not null, we solve the initial data identification problem for the equation (2.6) and target state v_T as in [14, 25]. We call $\mathcal{I}(v_T)$ the set of initial conditions leading to v_T at $t = T$.

Given v_0 in $\mathcal{I}(v_T)$, we consider its evolution $(t,x) \mapsto \mathcal{S}_t^+(v_0)(x) = v(t,x)$ and we set $Z_T = (z_1^T = u_1^T/v^T, z_2^T = u_2^T/v^T)$. Then we solve (2.7) backward from the final condition z_1^T and z_2^T, using v in the velocity coefficient. This produces a unique couple of initial data

$$\left(\bar{u}_1 = v_0 \mathscr{S}_T^-[v](z_1^T), \bar{u}_2 = v_0 \mathscr{S}_T^-[v](z_2^T)\right).$$

We observe that, by linearity,

$$z_2^T = \frac{u_2^T}{v^T} = 1 - \frac{u_1^T}{v^T}, \qquad \bar{u}_2 = v_0 \mathscr{S}_T^-[v](z_2^T) = v_0\left(1 - \mathscr{S}_T^-[v](z_1^T)\right).$$

The same procedure allows us to describe the set of inverse designs associated with a reachable target $(v_T, w_T) \in \mathfrak{A}_T(\mathbb{R})$ for the system (2.1). The results in [14] on the geometrical and topological properties of $\mathcal{I}(v_T)$ immediately imply the following theorem.

Theorem 2.3 (Characterization and properties of the set of inverse designs)**.**

1) *Given $U_T = (u_1^T, u_2^T) \in L^\infty(\mathbb{R}; \mathbb{R}_+^2)$ such that $V_T = (v_T = u_1^T + u_2^T, w_T = u_1^T - u_2^T) \in \mathsf{A}_T(\mathbb{R})$, the set of inverse design*

$$\mathfrak{i}(U_T) = \{U_0 = (u_1^0, u_2^0) \in L^\infty(\mathbb{R}; \mathbb{R}_+) \times L^\infty(\mathbb{R}; \mathbb{R}_+) : S_T^+(U_0) = U_T\}$$

can be characterized as follows:

$$\mathfrak{i}(U_T) = \left\{ \begin{aligned} &U_0 = (u_1^0, u_2^0) \in L^\infty(\mathbb{R}; \mathbb{R}_+) \times L^\infty(\mathbb{R}; \mathbb{R}_+) : \\ &\qquad u_1^0 + u_2^0 \in \mathcal{I}(v_T) \text{ and } u_i^0 = v_0 \mathscr{S}_T^-[\mathcal{S}_*(v_0)](u_i^T/v^T),\ i = 1, 2 \end{aligned} \right\}.$$

2) *Given $V_T = (v_T, w_T) \in \mathfrak{A}_T(\mathbb{R})$, the set of inverse design*

$$\mathfrak{I}(V_T) = \{V_0 \in L^\infty(\mathbb{R}) \times L^\infty(\mathbb{R}) : \mathfrak{S}_T^+(V_0) = V_T\}$$

can be characterized as follows:

$$\mathfrak{I}(V_T) = \{(v_0, w_0) \in L^\infty(\mathbb{R}) \times L^\infty(\mathbb{R}) :\ v_0 \in \mathcal{I}(v_T) \text{ and } w_0 = \mathscr{S}_T^-[\mathcal{S}_*(v_0)](w_T)\}.$$

In both of the above cases, the 1–to–1 correspondence between the elements of $\mathcal{I}(v_T)$ and the elements of $\mathfrak{i}(U_T)$ and $\mathfrak{I}(V_T)$, together with the results on $\mathcal{I}(v_T)$ proved in [14, Propositions 5.1 & 5.2] *yield the following properties:*

(T1) *the set $\mathfrak{I}(V_T)$ is closed with respect to the $L^1_{\mathrm{loc}} \times L^1_{\mathrm{loc}}$ topology;*
(T2) *the set $\mathfrak{I}(V_T)$ has empty interior with respect to the $L^1_{\mathrm{loc}} \times L^1_{\mathrm{loc}}$ topology;*
(G1) *the sets $\mathfrak{I}(V_T)$ and $\mathfrak{i}(U_T)$ reduce to a singleton if and only if $v_T \in C(\mathbb{R})$.*

To conclude this section, we recall following explicit characterization of $\mathcal{I}(v_T)$, which was first introduced in [25]

Theorem 2.4 (Inverse design for scalar conservation laws)**.** *Let us consider a strictly convex scalar conservation law of the form* (1.1)*, fix $T > 0$, and let $v_T \in \mathcal{A}_T(\mathbb{R}, f)$. Then, the initial data $\tilde{u}_0 \in L^\infty(\mathbb{R})$ verifies $\mathcal{S}_T^+(\tilde{u}_0) = u_T$ if and only if the following statement holds:*

1) *for any $(x, y) \in X(u_T) \times \mathbb{R}$*

$$\int_{x - T f'(u_T(x))}^{y} \mathcal{S}_T^-(u_T)(s)\,\mathrm{d}s \le \int_{x - T f'(u_T(x))}^{y} \tilde{u}_0(s)\,\mathrm{d}s, \tag{2.20}$$

2) *for any $(x, y) \in X(u_T)^2$*

$$\int_{x - T f'(u_T(x))}^{y - T f'(u_T(y))} \mathcal{S}_T^-(u_T)(s)\,\mathrm{d}s = \int_{x - T f'(u_T(x))}^{y - T f'(u_T(y))} \tilde{u}_0(s)\,\mathrm{d}s, \tag{2.21}$$

where $X(u_T)$ is the set of points of approximate continuity of u_T.

3. Unreachable profiles and optimization problem

In this section, we fix $T > 0$ and consider a target profile $V_{tar} = (v_{tar}, w_{tar})$ which is not attainable in time T for the system (2.1). We assume that $V_{tar} \in L^\infty(\mathbb{R}; \mathbb{R}^2)$ and that both of its components are constant outside a compact interval $[a, b]$, more precisely

$$v_{tar}(x) = \begin{cases} v^-, & \text{for } x < a, \\ \bar{v}(x), & \text{for } x \in [a, b], \\ v^+, & \text{for } x > b, \end{cases} \qquad w_{tar}(x) = \begin{cases} w^-, & \text{for } x < a, \\ \bar{w}(x), & \text{for } x \in [a, b], \\ w^+, & \text{for } x > b, \end{cases}$$

for some essentially bounded functions $\bar{v}, \bar{w}$. In the following we write C for $\|V_{tar}\|_{L^\infty(\mathbb{R})} = \max\{\|v_{tar}\|_{L^\infty(\mathbb{R})}, \|w_{tar}\|_{L^\infty(\mathbb{R})}\}$.

We want to characterize the initial conditions which drive the system as close as possible to V_{tar} with respect to the L^2 norm. These are the minima of

$$J_0(Q_0) = \|\mathfrak{S}_T^+(Q_0) - V_{tar}\|_{L^2(\mathbb{R};\mathbb{R}^2)},$$

where $\mathfrak{S}_T^+(Q_0)$ belongs to the subset of $\mathfrak{A}_T(\mathbb{R})$ defined as

$$\mathcal{U}^T(V_{tar}) = \left\{Q = (q_1, q_2) \in L^\infty(\mathbb{R};\mathbb{R}^2) :\ q_1 \in \mathcal{A}_T(\mathbb{R}, f),\ \|Q\|_{L^\infty(\mathbb{R})} \le C,\ \text{and } Q - V_{tar} \in L^1(\mathbb{R})\right\}.$$

Since the constants, such as $v^\pm$ and $w^\pm$, are always attainable, without loss of generality we can strengthen the last assumption and say that q_1, q_2 are constant, taking the values $v^\pm$ and $w^\pm$, outside a compact interval K containing $[a, b]$.

Due to the definition of $\mathfrak{A}_T$ in (2.17), this optimization problem is equivalent to the one studied in [25], namely finding $q_{1,\,\mathrm{opt}}$ such that

$$\|q_{1,\,\mathrm{opt}} - v_{tar}\|_{L^2(\mathbb{R})} = \min_{q \in \mathcal{U}_1^T(V_{tar})} \|q - v_{tar}\|_{L^2(\mathbb{R})}\,, \tag{3.1}$$

where the admissible set $\mathcal{U}_1^T(V_{tar})$ is defined by

$$\mathcal{U}_1^T(V_{tar}) = \left\{q \in L^\infty(\mathbb{R}) :\ q \in \mathcal{A}_T\left(\mathbb{R}, v \mapsto \frac{v}{1+v}\right),\ \|q\|_{L^\infty(\mathbb{R})} \le C,\ \text{and } \operatorname{supp}(q - v_{tar}) \subset K\right\}.$$

It has been shown in [25, Theorem 2.1] that $q_{1,\,\mathrm{opt}} = \mathcal{S}_T^+(\mathcal{S}_T^-(v_{tar}))$.

Remark 3.1. *To be more precise, the statement of* [25, Theorem 2.1] *focuses on the set of initial conditions eventually leading to $q_{1,\,opt}$ in time T, and which L^∞-norm is bounded by the L^∞-norm of the non-reachable target v_{tar}. However, this second condition seems not to be necessary (the L^∞-norm of the solution to scalar conservation laws may decrease during the evolution). The proof consists of two steps:*

1. *proving that $q_{1,\,opt}$ is the solution to the minimization problem* (3.1)*;*
2. *applying the characterization of $\mathcal{I}(q_{1,\,opt})$ from Theorem 2.4.*

It should be noticed, however, that $(q_{1,\,\mathrm{opt}}, w_{tar})$ does not necessarily belong to $\mathsf{A}_T(\mathbb{R})$ as $q_{1,\,\mathrm{opt}} - w_{tar}$ is not everywhere positive.

Therefore, if we fix $T > 0$ and consider a target profile $U_{tar} = (u_1^{tar}, u_2^{tar}) \in L^\infty(\mathbb{R}, \mathbb{R}_+^2)$ which is not attainable in time T for the system (1.2), we need to slightly modify the problem above and its solution.

First, we associate to U_{tar} the profile $V_{tar} = (v_{tar} = u_1^{tar} + u_2^{tar}, w_{tar} = u_1^{tar} - u_2^{tar})$. Then we apply the strategy above to find $q_{1,\,\mathrm{opt}}$. Finally, we consider $q_{2,\,\mathrm{opt}} = \min\{q_{1,\,\mathrm{opt}}, w_{tar}\}$ so to obtain a second component which is as close as possible to w_{tar}, under the constraint that $q_{1,\,\mathrm{opt}} - q_{2,\,\mathrm{opt}} \ge 0$. The couple $Q_{\mathrm{opt}} = (q_{1,\,\mathrm{opt}}, q_{2,\,\mathrm{opt}})$ is in $\mathsf{A}_T(\mathbb{R})$, so that the profile attainable at time T for (1.2) which is the closest to U_{tar} in L^2 is

$$U_{\mathrm{opt}} = \left(\frac{1}{2}(q_{1,\,\mathrm{opt}} + q_{2,\,\mathrm{opt}}),\ \frac{1}{2}(q_{1,\,\mathrm{opt}} - q_{2,\,\mathrm{opt}})\right).$$

The following numerical examples are designed to illustrate the above considerations.

Example 3.1 (Optimization problem)**.** *Given the initial conditions $V_0 = (v_0, w_0)$, with*

$$v_0(x) = \begin{cases} 0.5, & \text{if } -1 < x < 0, \\ 0.25, & \text{otherwise}, \end{cases} \qquad w_0(x) = \begin{cases} 0.5, & \text{if } -1 < x < 0, \\ 0.15, & \text{otherwise}, \end{cases}$$

we let them evolve for time $t = 3/4$ and we consider as target profile at time 1, $V_{tar} = \mathfrak{S}_{3/4}^+(V_0) = (v_{tar}, w_{tar})$. The profile v_{tar} does not belong to $\mathcal{A}_1(\mathbb{R}, v/(1+v))$ because the evolution of the piecewise constant profile v_0 is a rarefaction wave (which is isentropic), so that $\mathcal{S}_{3/4}^-(v_{tar}) = \mathcal{S}_{3/4}^-\left(\mathcal{S}_{3/4}^+(v_0)\right) = v_0$, which means that backward characteristics focus at one point at $T = 1/4$, before reaching $T = 0$.

There are a few attainable profiles that are very natural to compare to V_{tar}.

1. *From the construction above it is evident that $\mathfrak{S}_{1/4}^+(V_{tar}) = \mathfrak{S}_1^+(V_0)$ belongs to $\mathsf{A}_1(\mathbb{R})$.*

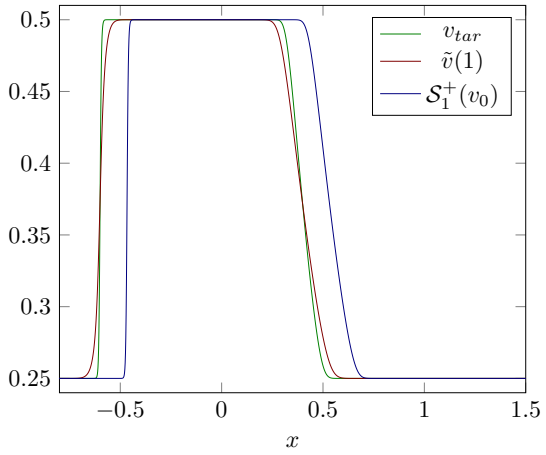

FIGURE 1. The profiles v_{tar}, $\tilde{v}(1,\cdot)$ and $\mathcal{S}_1^+(v_0)$.

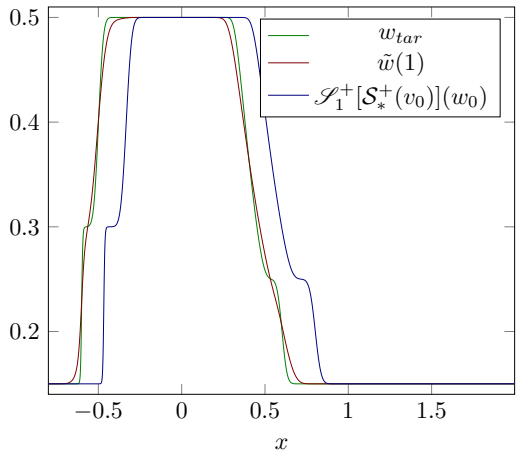

FIGURE 2. figure
The profiles w_{tar}, $\tilde{w}(1)$ and $\mathscr{S}_1^+[\mathcal{S}_*^+(v_0)](w_0)$.

(2) *Following the procedure in* [25]*, we apply the backward and the forward semigroups to* v_{tar}

$$\mathcal{S}_t^+\left(\mathcal{S}_1^-(v_{tar})\right) = \tilde{v}(t,\cdot).$$

The function $\tilde{v}$ *satisfies*

$$\|\tilde{v}(1,\cdot) - v_{tar}\|_{L^2(\mathbb{R})} = \min_{s\in\mathcal{A}_1(\mathbb{R},v/(1+v))} \|s - v_{tar}\|_{L^2(\mathbb{R})}. \tag{3.2}$$

In particular, we can observe that the shock in $\tilde{v}$ *is exactly in the same location as the one in* v_{tar}*. We can use* $\tilde{v}$ *to construct an attainable profile for the system in the following three ways.*

(a) *We apply an analogous backward-forward approach to the transport equation and compute*

$$\mathscr{S}_t^+[\tilde{v}]\left(\mathscr{S}_1^-\left[\mathcal{S}_*^-(v_{tar})\right](w_{tar})\right) = \tilde{w}(t,\cdot).$$

The profile $\tilde{V} = (\tilde{v}(1,\cdot), \tilde{w}(1,\cdot))$ *is in* $\mathfrak{A}_1(\mathbb{R})$*.*

(b) *Since* $w_{tar} \in L^\infty(\mathbb{R})$*, the profile* $\bar{V} = (\tilde{v}(1,\cdot), w_{tar}) \in \mathfrak{A}_1(\mathbb{R})$*. However, this couple does not belong to* $\mathsf{A}_1(\mathbb{R})$ *as* $\tilde{v}(1,\cdot) - w_{tar}$ *is not everywhere positive, see Figure 3.*

(c) *We can define* $w_{\min}(x) = \min\{\tilde{v}(1,x), w_{tar}(x)\}$ *and take* $V_{\min} = (\tilde{v}(1,\cdot), w_{\min}) \in \mathsf{A}_1(\mathbb{R})$*.*

In this simple example, we can compute numerically all the profiles above and their L^2*-distance from* V_1*. For the computation, we take* $\Delta x = 7.8 \times 10^{-4}$ *and* $\Delta t = \Delta x/2$*. The closest profile in* $\mathfrak{A}_1(\mathbb{R})$ *is* $\bar{V}$*, while the closest one in* $\mathsf{A}_1(\mathbb{R})$ *is* $V_{\min}$*.*

4. Boundary controllability via Lyapunov methods

In this section, we consider the evolution of the system (2.1) in a bounded interval, $(0, L)$.

$$\begin{cases} \partial_t v + \partial_x\left(\dfrac{v}{1+v}\right) = 0, & t>0,\ x\in(0,L), \\ \partial_t w + \partial_x\left(\dfrac{w}{1+v}\right) = 0, & t>0,\ x\in(0,L), \\ v(0,x) = v_0(x), & x\in(0,L), \\ w(0,x) = w_0(x), & x\in(0,L), \\ v(t,0) = v_b(t), & t>0, \\ w(t,0) = w_b(t), & t>0. \end{cases} \tag{4.1}$$

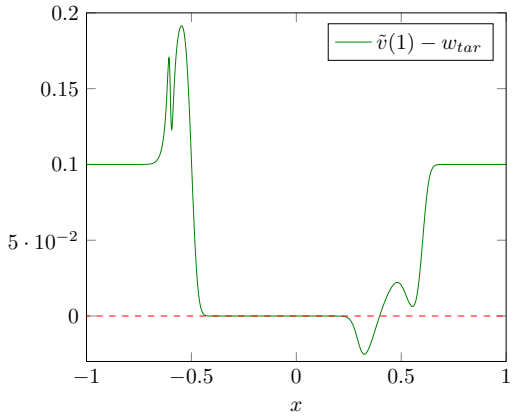

FIGURE 3. The function $\tilde{v}(1,\cdot) - w_{tar}$ is not everywhere positive.

p	r	$\|p-r\|_{L^2}$
v_{tar}	$\tilde{v}(1)$	0.01469
v_{tar}	$\mathcal{S}_1^+(v_0)$	0.10972
w_{tar}	$\tilde{w}(1)$	0.01417
w_{tar}	$\mathscr{S}_1^+[\mathcal{S}_*^+(v_0)](w_0)$	0.12873
$\min\{\tilde{v}(1), w_{tar}\}$	w_{tar}	0.00624

TABLE 1. Distances in the L^2 norm.

We rely on the well-posedness results for the initial boundary value problem established by Choudhury, Crippa, and Spinolo in [13]. In particular, to ensure the existence of a unique renormalized entropy solution $(v,w) \in L^\infty(\mathbb{R}_+ \times (0,L);(\mathbb{R}_+)^2)$ we need to assume that both the initial and the boundary conditions are not only essentially bounded, but also of bounded variation: $(v_0,w_0) \in L^\infty((0,L);(\mathbb{R}_+)^2) \cap \mathrm{BV}((0,L);(\mathbb{R}_+)^2)$, $(v_b,w_b) \in L^\infty(\mathbb{R}_+;(\mathbb{R}_+)^2) \cap \mathrm{BV}(\mathbb{R}_+;(\mathbb{R}_+)^2)$.

An important ingredient of the analysis in [13] is a trace renormalization result, namely [13, Theorem 2.2], originally proved in [6]. In our simple setting, it reduces to the fact that if $v \in L^\infty(\mathbb{R}_+ \times (0,L);\mathbb{R}_+) \cap \mathrm{BV}(\mathbb{R}_+ \times (0,L);\mathbb{R}_+)$ and $z \in L^\infty(\mathbb{R}_+ \times (0,L);\mathbb{R}_+)$ are such that $(v, w = vz)$ provides a renormalized entropy solution to (4.1), then, for any given $h \in C^1(\mathbb{R})$ and C^2-curve $t \mapsto (t,\gamma(t))$ in $\mathbb{R}_+ \times [0,L]$ we have

$$\mathrm{tr}^\pm(h(z)v,\gamma(t)) = h\left(\frac{\mathrm{tr}^\pm(zv,\gamma(t))}{\mathrm{tr}^\pm(v,\gamma(t))}\right)\mathrm{tr}^\pm(v,\gamma(t)), \tag{4.2}$$

where the value of $\dfrac{\mathrm{tr}^\pm(zv,\gamma(t))}{\mathrm{tr}^\pm(v,\gamma(t))}$ can be set arbitrarily whenever $\mathrm{tr}^\pm(v,\gamma(t))$ vanishes.

Our final theorem concerns the boundary controllability to trajectories of (4.1). We can impose boundary conditions only at $x = 0$ due to the strict increasing monotonicity of the fluxes. In the following, we call

$$f(\xi) = \frac{\xi}{1+\xi}, \qquad g(\xi) = \frac{1}{1+\xi}.$$

Proposition 4.1 (Finite-time stabilization)**.** *Given a couple of entropy solutions of* (4.1) (v,w) *and* $(\bar v,\bar w)$ *corresponding respectively to the initial conditions* (v_0,w_0), $(\bar v_0,\bar w_0) \in L^\infty((0,L);(\mathbb{R}_+)^2) \cap \mathrm{BV}((0,L);(\mathbb{R}_+)^2)$, *and the common boundary data* $(v_b,z_b) \in L^\infty(\mathbb{R}_+;(\mathbb{R}_+)^2) \cap \mathrm{BV}(\mathbb{R}_+;(\mathbb{R}_+)^2)$, *we have that for any* $T > \bar T := L/c$, $v(T,x) = \bar v(T,x)$ *and* $w(T,x) = \bar w(T,x)$ *for a.e.* $x \in (0,L)$ *with*

$$c := \inf_{\xi\in[0,\bar M]} f'(\xi) := \inf_{\xi\in[0,\bar M]} (\xi/(1+\xi))' = \inf_{\xi\in[0,\bar M]} 1/(1+\xi)^2, \tag{4.3}$$

where $\bar M := \max\{\sup_{(0,L)} v_0, \sup_{(0,L)} \bar v_0, \sup_{[0,T]} v_b\}$.

Proof of Proposition 4.1. This result is classical for hyperbolic systems of conservation laws. It suffices to notice that the eigenvalues of the two (genuinely nonlinear) characteristic families of the system in (4.1) are $\lambda_1(\xi,\zeta) = f'(\xi)$ and $\lambda_2(\xi,\zeta) = g(\xi)$. From the analytical expression of f and g, we have that $\lambda_1(\xi,\zeta) \le \lambda_2(\xi,\zeta)$. The system is not strictly hyperbolic, so that for the umbilical value $\xi = 0$ the two eigenvalues take 1 as the common value. However, as soon as we have at our disposal an upper bound

for ξ, as it is $\bar{M}$ in our case, the propagation speed of all waves in any Riemann problem is bounded from below by $c = \inf_{\xi\in[0,\bar{M}]} f'(\xi)$. Therefore any two solutions of the initial boundary value problem (4.1) coincides in the triangular region $\mathcal{T} = \{(t,x) \in \mathbb{R}^2 : t \geq 0,\ 0 \leq x \leq tc\}$.

Since $\bar{T}$ is defined as L/c, this is enough to prove the theorem. □

Corollary 4.1 (Boundary controllability to trajectories)**.** *Let $(\tilde{v},\tilde{w})$ be a solution of (4.1) with initial data $(\tilde{v_0},\tilde{w_0}) \in L^\infty((0,L);(\mathbb{R}_+)^2) \cap \mathrm{BV}((0,L);(\mathbb{R}_+)^2)$ and boundary data $(\tilde{v}_b,\tilde{w}_b) \in L^\infty(\mathbb{R}_+;(\mathbb{R}_+)^2) \cap \mathrm{BV}(\mathbb{R}_+;(\mathbb{R}_+)^2)$. For any $(v_0,w_0) \in L^\infty((0,L);(\mathbb{R}_+)^2) \cap \mathrm{BV}((0,L);(\mathbb{R}_+)^2)$ and $T_1,T_2 \geq \bar{T} := L/c$, there exists a boundary control $(v_b,w_b) \in L^\infty(\mathbb{R}_+;(\mathbb{R}_+)^2) \cap \mathrm{BV}(\mathbb{R}_+;(\mathbb{R}_+)^2)$ which leads to a solution (v,w) satisfying*

$$(v,w)(0,x) = (v_0,w_0)(x), \qquad (v,w)(T_1,x) = (\tilde{v},\tilde{w})(T_2,x), \qquad \text{for a.e. } x \in (0,L).$$

Proof of Corollary 4.1. Following the strategy in [17], we split the proof into two cases to build suitable boundary data (controls) steering (v,z) to $(\tilde{v},\tilde{z})$.

Case 1: $T_2 \geq T_1$**.**

We solve the IBVP (4.1) for the data $(\tilde{v_0},\tilde{w_0})$ and $(\tilde{v}_b,\tilde{w}_b)$ in $[0,T_2]\times(0,L)$. Then we use the genuine nonlinearity of f and the trace renormalization formula (4.2) to motivate the definition of the auxiliary function

$$s \mapsto U_b(s) = (h_b(s),\ell_b(s)) := \Big(\tilde{v}\left(T_2 - T_1 + s, 0^+\right),\ \tilde{w}\left(T_2 - T_1 + s, 0^+\right)\Big),$$

and we consider the IBVP

$$\begin{cases} \partial_t h(s,x) + \partial_x f(h(s,x)) = 0, & (s,x) \in (0,T_1)\times(0,L), \\ \partial_t \ell(s,x) + \partial_x \left(g(h(s,x))\ell(s,x)\right) = 0, & (s,x) \in (0,T_1)\times(0,L), \\ h(0,x) = \tilde{v}\left(T_2 - T_1, x\right), & x \in (0,L), \\ \ell(0,x) = \tilde{w}\left(T_2 - T_1, x\right), & x \in (0,L), \\ h(s,0) = h_b(s), & s \geq 0, \\ \ell(s,0) = \ell_b(s), & s \geq 0. \end{cases} \tag{4.4}$$

The unique renormalized entropy solution of (4.4) is given by

$$U(s,x) = \Big(h(s,x) = \tilde{v}\left(T_2 - T_1 + s, x\right),\ \ell(s,x) = \tilde{w}\left(T_2 - T_1 + s, x\right)\Big).$$

By Proposition 4.1, we deduce that the IBVP (4.1) with initial conditions (v_0,w_0) and boundary condition U_b admits a unique renormalized entropy solution (v,w), which satisfies (since $T_1 \geq \bar{T}$)

$$v\left(T_1,x\right) = h\left(T_1,x\right), \qquad w\left(T_1,x\right) = \ell\left(T_1,x\right) \qquad x \in (0,L),$$

which means

$$v\left(T_1,x\right) = \tilde{v}\left(T_2,x\right), \qquad w\left(T_1,x\right) = \tilde{w}\left(T_2,x\right), \qquad x \in (0,L).$$

Case 2: $T_1 \geq T_2$**.**

We solve the IBVP (4.1) for the data $(\tilde{v_0},\tilde{w_0})$ and $(\tilde{v}_b,\tilde{w}_b)$ in $[0,T_1]\times(0,L)$. Then we use the genuine nonlinearity of f and the trace renormalization formula (4.2) to motivate the definition of the auxiliary function

$$s \mapsto \bar{U}_b(s) = (\bar{h}_b(s),\bar{\ell}_b(s)) := \left(\tilde{v}\left(T_2 - \bar{T} + s, 0^+\right), \tilde{w}\left(T_2 - \bar{T} + s, 0^+\right)\right),$$

and we consider the IBVP

$$\begin{cases} \partial_t h(s,x) + \partial_x f(h(s,x)) = 0, & (s,x) \in (0,T_1)\times(0,L), \\ \partial_t \ell(s,x) + \partial_x \left(g(h(s,x))\ell(s,x)\right) = 0, & (s,x) \in (0,T_1)\times(0,L), \\ h(0,x) = \tilde{v}\left(T_2 - \bar{T}, x\right), & x \in (0,L), \\ \ell(0,x) = \tilde{w}\left(T_2 - \bar{T}, x\right), & x \in (0,L), \\ h(s,0) = \bar{h}_b(s), & s \geq 0, \\ \ell(s,0) = \bar{\ell}_b(s), & s \geq 0. \end{cases} \tag{4.5}$$

We have that the unique renormalized entropy solution of (4.5) is given by

$$\bar{U}(s,x) = \left(h(s,x) = \tilde{v}\left(T_2 - \bar{T} + s, x\right), \ell(s,x) = \tilde{w}\left(T_2 - \bar{T} + s, x\right)\right).$$

Given any couple of constant values μ_1 and $\mu_2 \in [0, \bar{M}]$, we can solve the IBVP (4.1) with the initial condition (v_0, w_0) and the constant boundary conditions (μ_1, μ_2) on $[0, T_1 - \bar{T}] \times (0, L)$. We call $V^* = (v^*, w^*)$ the unique renormalized entropy solutions obtained. We use its profile at time $t = T_1 - \bar{T}$ as the initial condition to the IBVP

$$\begin{cases} \partial_t h^*(s,x) + \partial_x f(h^*(s,x)) = 0, & (s,x) \in (0,T_1) \times (0,L), \\ \partial_t \ell^*(s,x) + \partial_x \left(g(h^*(s,x))\ell^*(s,x)\right) = 0, & (s,x) \in (0,T_1) \times (0,L), \\ h^*(0,x) = v^*(T_1 - \bar{T}, x), & x \in (0,L), \\ \ell^*(0,x) = w^*(T_1 - \bar{T}, x), & x \in (0,L), \\ h^*(s,0) = \bar{h}_b(s), & s \geq 0, \\ \ell^*(s,0) = \bar{\ell}_b(s), & s \geq 0. \end{cases} \tag{4.6}$$

Applying Proposition 4.1 yields that the renormalized entropy solutions of (4.5) and (4.6) coincide for all times $t \geq \bar{T}$. This means that by using the given initial condition (v_0, w_0) and the boundary conditions

$$t \mapsto (v_b(t), w_b(t)) = \begin{cases} (\mu_1, \mu_2), & 0 < t \leq T_1 - \bar{T}, \\ \bar{U}_b(t), & \text{otherwise}, \end{cases}$$

we obtain a renormalized entropy solution (v, w) of (4.1) such that

$$v(T_1, x) = \tilde{v}(T_2, x), \qquad w\left(T_1, x\right) = \tilde{w}\left(T_2, x\right), \qquad x \in \mathbb{R}.$$

□

Example 4.1 (Controllability to trajectories)**.** *In Figures 4,5,6, and 7, we present a numerical experiment illustrating Case 2 of the proof of the Corollary 4.1: $T_1 > T_2$. We fix $L = 1$, $\bar{T} = 2.89$, $T_2 = \bar{T} + 1$, $T_1 = T_2 + 1$, $\mu_1 = 0.4$ and $\mu_2 = 0.25$, consider the initial conditions*

$$v_0(x) = 0.5 + 0.2\sin(2\pi x), \qquad \bar{v}_0(x) = \begin{cases} 0.5, & \textit{for } x < 0.25, \\ 0.8 \times (x - 0.25) + 0.35, & \textit{for } x \in [0.25, 0.75], \\ 0.6, & \textit{otherwise}, \end{cases} \tag{4.7}$$

$$w_0(x) = 0.2 + 0.1\cos(2\pi x), \qquad \bar{w}_0(x) = \begin{cases} 0.45, & \textit{for } x < 0.15, \\ -1.5 \times (x - 0.15) + 0.45, & \textit{for } x \in [0.15, 0.3[, \\ 0.225, & \textit{for } x \in [0.3, 0.5[, \\ 0.4 - 0.1\sin(4\pi x), & \textit{otherwise}, \end{cases} \tag{4.8}$$

and the boundary controls

$$\bar{v}_b(t) = 0.3 + 0.2\cos(\pi t), \qquad \bar{w}_b(t) = \frac{(0.3 + 0.2\cos(\pi t)) \times |\sin(2\pi t)|}{1.5}. \tag{4.9}$$

In Figure 7, we show at the same scale the portion of the evolution of v and $\bar{v}$ in which they have the same boundary conditions.

5. Numerical analysis

In this section, we present some results on the numerical backward reconstruction of system (2.1) on $[0, T] \times J$, where J is a given closed interval $[A_1, A_2] \subset \mathbb{R}$, $A_1 < A_2$, $T > 0$ and where the final state $V_T = (v_T, w_T)$ belongs to $\mathcal{A}_T \times L^\infty(J)$.

Let us describe the numerical method:

(1) first, we use the entropic solver for the backward problem (2.15), which gives the isentropic solution of the first equation;

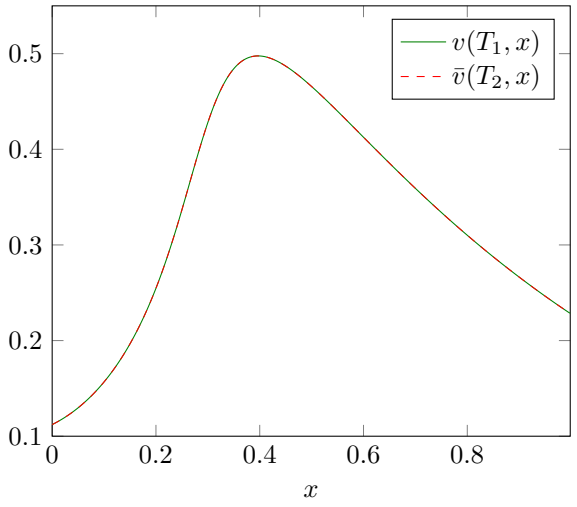

FIGURE 4. Profile v at time T_1 and $\bar{v}$ at time T_2.

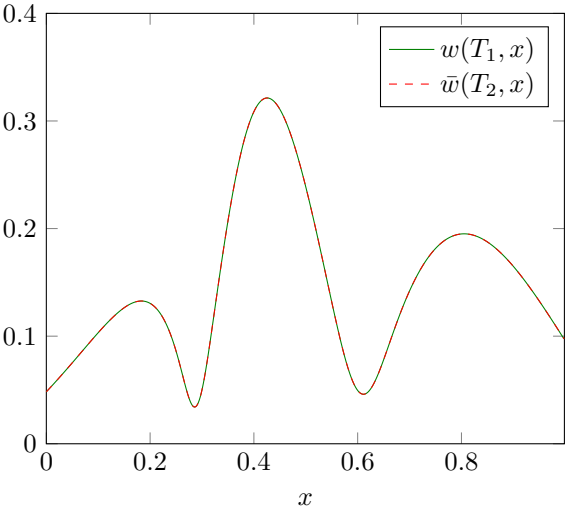

FIGURE 5. Profile w at time T_1 and $\bar{w}$ at time T_2.

(2) then, the numerical backward resolution of the transport equation is based on considering the auxiliary forward problem

$$\partial_t w + \partial_x \left(-g(v)w\right) = 0, \qquad t > 0,\ x \in \mathbb{R}, \tag{5.1}$$

where v is an entropic solution of the first equation.

To perform the computations, we need to determine the domain of dependence of the system, which is given by $I = [C_1, C_2]$, where

$$C_1 = \min\{A_1, B_{1,1}, B_{2,1}\}, \quad C_2 = \max\{A_2, B_{1,2}, B_{2,2}\},$$

and

$$\begin{aligned} B_{1,1} &= A_1 - Tf'(v_T(A_1)), & B_{1,2} &= A_2 + Tf'(v_T(A_2)), \\ B_{2,1} &= A_1 - Tg(v_T(A_1)), & B_{2,2} &= A_2 + Tg(v_T(A_2)). \end{aligned}$$

We shall rely on a finite volume scheme. We introduce a regular grid,

$$C_1 = x_{1/2} < x_{3/2} < \cdots < x_{m-1/2} < x_{m+1/2} = C_2,$$

and define the cells $K_j = [x_{j-1/2}, x_{j+1/2}]$ with centers at $x_j = \frac{1}{2}(x_{j-1/2} + x_{j+1/2})$, for $1 \le j \le m$, and a constant space step $\Delta x = x_{3/2} - x_{1/2}$. We define a time discretization $(t^n)_{n=0}^{N+1}$, where $t^0 = 0$, $t^{N+1} = T$, and $t^n = n\Delta t$ for a constant time-step Δt.

With this notation in place, we define v_j^n and w_j^n as the approximations of the averages $v(t^n, \cdot)$ and $w(t^n, \cdot)$ on K_j. Namely,

$$\begin{aligned} v_j^n &\simeq \frac{1}{\Delta x}\int_{K_j} v(t^n, x)\,\mathrm{d}x, & w_j^n &\simeq \frac{1}{\Delta x}\int_{K_j} w(t^n, x)\,\mathrm{d}x, \\ v_j^{N+1} &\simeq \frac{1}{\Delta x}\int_{K_j} v(T, x)\,\mathrm{d}x, & w_j^{N+1} &\simeq \frac{1}{\Delta x}\int_{K_j} w(T, x)\,\mathrm{d}x. \end{aligned}$$

For the first equation, we consider the numerical backward solver $\mathcal{K}^{-,n}\left(v_T, (x_j)_{j=1}^M\right) = (v_j^{N+1-n})_{j=1}^M$, which gives us an approximation of of the semigroup $\mathcal{K}^-$, i.e. of the isentropic solution of the first equation, such that

$$v_j^n = v_j^{n+1} - \frac{\Delta t}{\Delta x}\left(\mathcal{F}(v_j^{n+1}, v_{j-1}^{n+1}) - \mathcal{F}(v_{j+1}^{n+1}, v_j^{n+1})\right),$$

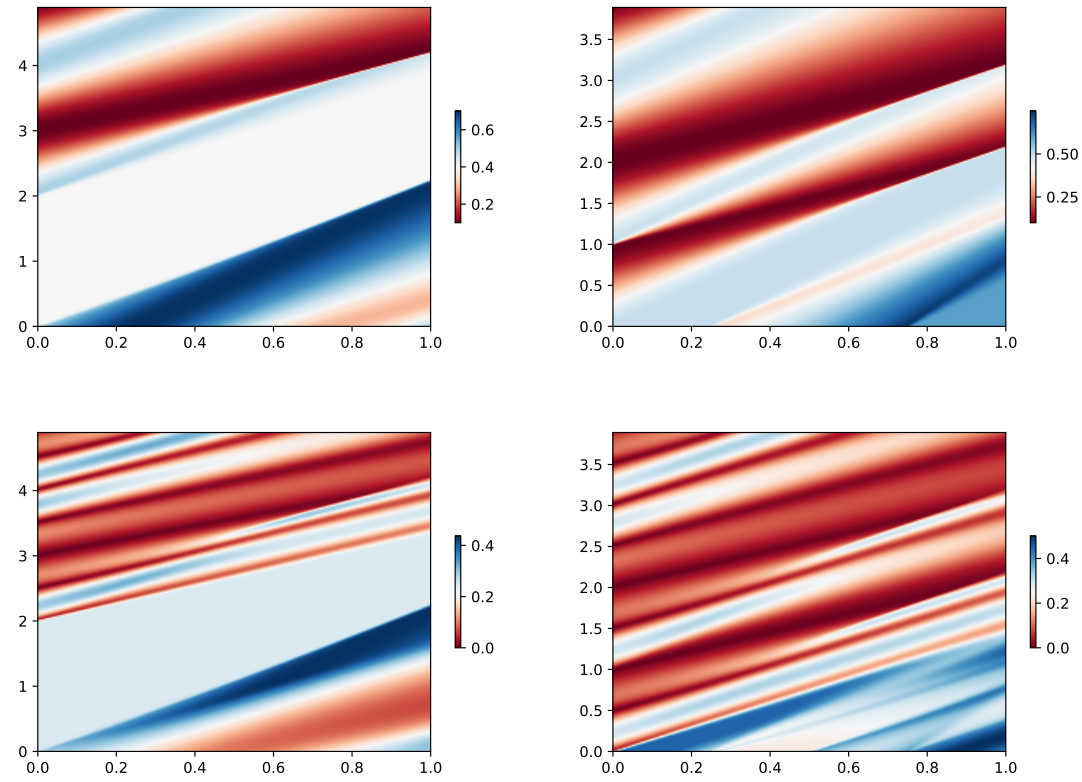

FIGURE 6. Left: the evolution of the component v (top) and w (bottom) of the solution of (4.1) on $[0, T_1] \times (0, 1)$ with initial data (v_0, w_0) as in (4.7)–(4.8) and boundary control given by the strategy of Corollary 4.1.
Right: the evolution of the component $\bar{v}$ (top) and $\bar{w}$ (bottom) of the solution of (4.1) on $[0, T_2] \times (0, 1)$ with initial data $(\tilde{v}_0, \tilde{w}_0)$ as in (4.7)–(4.8) and boundary control given by (4.9).

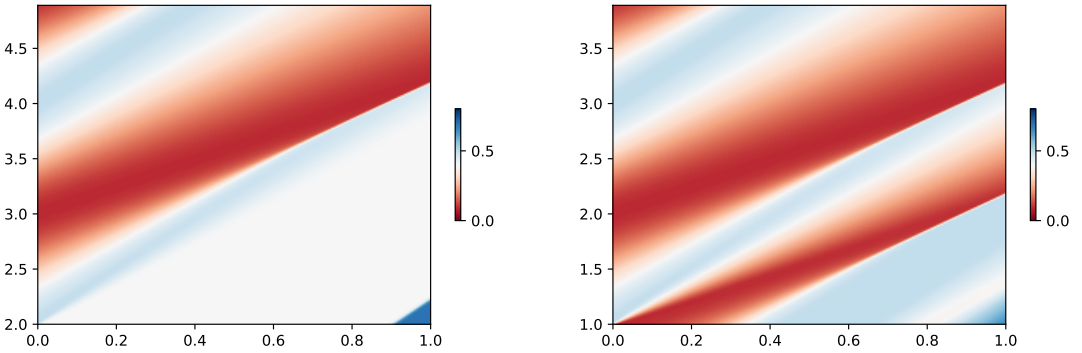

FIGURE 7. Zoom of the evolution of v and $\bar{v}$ (from Figure 6) in the time interval in which they share the same boundary conditions.

$\mathcal{F}$ being the *Godunov numerical flux* (see [19, 24])

$$\mathcal{F}(v_l, v_r) = \begin{cases} \min\limits_{v\in[v_l,v_r]} f(v), & \text{if } v_l \le v_r, \\ \max\limits_{v\in[v_l,v_r]} f(v), & \text{otherwise.} \end{cases}$$

Then, $\mathcal{K}^{-,n}\left(v_T, (x_j)_{j=1}^M\right) = (\mathcal{K}^{+,n}\left(v_T \circ r, (x_j)_{j=1}^M\right)$ gives us the approximation of the isentropic solution of the first equation.

Having obtained v_j^n, we then update w_j^n by using an upwind-type scheme (see [20]):

$$\begin{aligned} w_j^n = w_j^{n+1} - \frac{\Delta t}{\Delta x}[\{(-g_{j+1/2}^{n+1})^+ w_j^{n+1} - (-g_{j-1/2}^{n+1})^+ w_{j-1}^{n+1}\} \\ + \{(-g_{j+1/2}^{n+1})^- w_{j+1}^{n+1} - (-g_{j-1/2}^{n+1})^- w_j^{n+1}\}], \end{aligned}$$

where

$$g_{j+1/2}^{n+1} = (1-\theta) g(v_j^{n+1}) + \theta g(v_{j+1}^{n+1}),$$

where $\theta \in (0,1)$ (in particular, for the numerical simulations in Section 5.1, we take $\theta = 1/2$), $\xi^+ = \max\{0,\xi\}$, and $\xi^- = \min\{0,\xi\}$.

For the boundary conditions, we set

$$(v_1^n, w_1^n) = (v_T(A_1), w_T(A_1)), \quad (v_M^n, w_M^n) = (v_T(A_2), w_T(A_2)), \quad 1 \le n \le N+1.$$

This procedure yields the isentropic solution $V = (v, w)$ of the system corresponding to the attainable profile $V_T = (v_T, w_T)$.

In order to find other initial data leading to V_T, we rely on Theorem 2.4, which gives a geometrical way to describe the set of initial states which leads to the state v_T (cf. [26]).

Remark 5.1 (Geometric interpretation of Theorem 2.4)**.** *Let v_T an admissible state for the conservation law in* (2.1)*, with a discontinuity at $\overline{x} \in \mathbb{R}$, $v_L < v_R$ such that $v_T(\overline{x}^-) = v_L$ and $v_T(\overline{x}^+) = v_R$, $T > 0$ and $f : v \mapsto \frac{v}{1+v}$. We introduce the notation $B_L^T = \overline{x} - Tf'(v_L)$ and $B_R^T = \overline{x} - Tf'(v_R)$. We call D_T the interval $[B_L^T, B_R^T]$. We introduce the set $\Gamma(v_L, v_R, \overline{x}, T)$ such that $\gamma \in \Gamma(v_L, v_R, \overline{x}, T)$ if*

1. *$\gamma : D_T \to \mathbb{R} \in W^{1,1}(\mathbb{R})$;*
2. *$\gamma' \in \mathrm{BV}(D_T)$ the space of functions with bounded variations;*
3. *$\gamma(B_L^T) = 0$;*
4. *$\gamma(B_R^T) = T(v_L f'(v_L) - f(v_L) - u_R f'(v_R) + f(v_R))$;*
5. *for every $x \in D_T$,*

$$\gamma(x) \ge \gamma_*(x) = -T \int_{v_L}^{(f')^{-1}\left(\frac{\overline{x}-x}{T}\right)} s f''(s)\,\mathrm{d}s;$$

6. *for every $x \in D_T, 0 < \gamma'(x) \le 1$.*

Then, to find an initial state $\tilde{v}_0$, we pick a path $\gamma \in \Gamma(v_L, v_R, \overline{x}, T)$, and the initial data $\tilde{v}_0$ corresponding to γ is defined by

$$\tilde{v}_0(x) = \begin{cases} \gamma'(x), & \text{for a.e. } x \in D_T, \\ v_0(x), & \text{for every } x \notin D_T, \end{cases}$$

where v_0 is the isentropic solution. Then, we know $\tilde{v}$ for almost every $(t,x) \in [0,T] \times \mathbb{R}$.

In light of Theorem 2.4 and Remark 5.1, we have a new profile $\tilde{v}$, which we can use to solve the second equation backward and obtain, in conclusion, another set of initial data $\tilde{V}_0 = (\tilde{v}_0, \tilde{w}_0)$ that leads to V_T.

The convergence results in [20] for the upwind scheme described above hold in the more general framework of duality solution for one-dimensional transport and continuity equations with discontinuous coefficients (see [11]).

For systems endowed with the very special structure we are considering in this paper the convergence to a duality solution of the second equation is equivalent to the convergence to its unique generalized

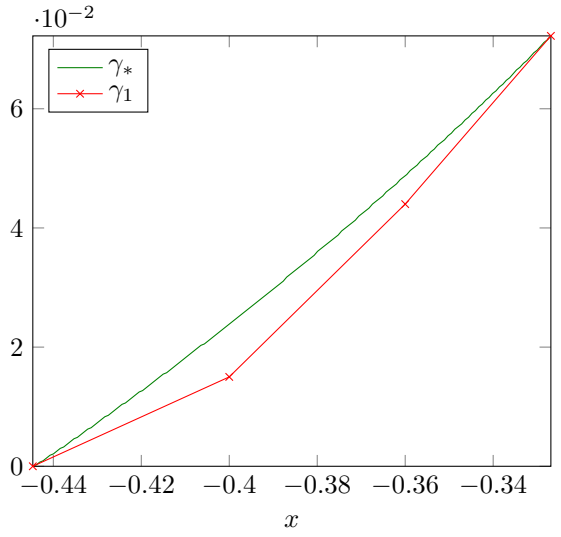

FIGURE 8. Paths γ_* and γ_1 leading to v_0 and $\tilde{v}_0$.

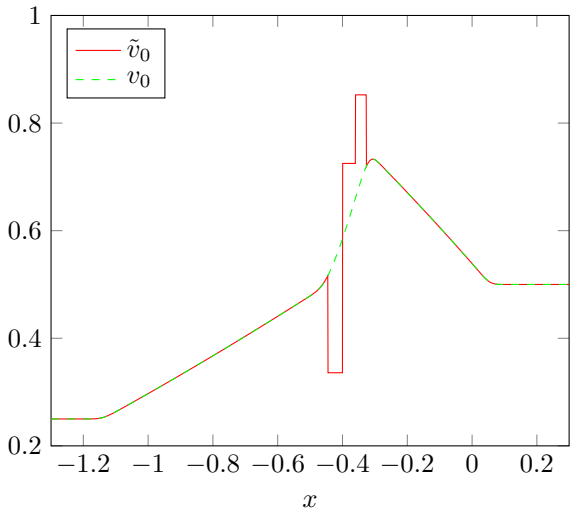

FIGURE 9. Initial data v_0 and $\tilde{v}_0$.

solution in the sense of Panov. We can recall, in passing, that in [9] the numerical scheme above was also applied to resonant systems (see Theorem 2.1) in cases where the DiPerna–Lions theory does not provide uniqueness for the second equations.

5.1. **Numerical experiments.** We now present a numerical experiment illustrating the backward reconstruction of (2.1) posed on the domain $[0,1]\times[-2,2]$. We consider

$$v_T(x)=\begin{cases}0.25, & \text{if } x<-0.5,\\ 0.25+0.5(x+0.5), & \text{if } -0.5\le x<0,\\ 0.75-0.5, & \text{if } 0\le x<0.5,\\ 0.5, & \text{if } 0.5\le x,\end{cases}$$

as a final state for the conservation law and

$$w_T(x)=\begin{cases}0.1, & \text{if } x\le -1,\\ 0.25(x+1)+0.1, & \text{if } -1<x\le 0,\\ 0.25(x-1)+0.4, & \text{if } 0<x\le 1,\\ 0.4, & \text{if } 1<x,\end{cases}$$

as a final state for the transport equation. We choose $\Delta x=7.8\times 10^{-4}$ and $\Delta t=\Delta x/2$.

First of all, we construct a random path $\gamma_1\in\Gamma(0.5,0.75,0,1)$ and perform the backward algorithm for v_T described in the previous section, which leads us to the initial state $\tilde{v}_0$ in Figure 9.

The iterative construction to have a random path is initiated with $(X_0,Y_0)=(\overline{x}-Tf'(v_L),0)$. Then, we construct randomly $(X_i,Y_i)_{i=1,\dots,k-2}$, where k is the number of jumps that we want, such that for all i, $X_i<X_{i+1}$. For $(Y_i)_{i=1,\dots,k-2}$ we pick randomly Y_{i+1} such that $0<\frac{Y_{i+1}-Y_i}{X_{i+1}-X_i}\le 1$, the line with slope $\frac{Y_{i+1}-Y_i}{X_{i+1}-X_i}$ have to be below $\gamma_*(x)$ for $x\in[X_i,X_{i+1}]$ and $Y_i\ge\min\{0,-(X_i-B_R^T)+\gamma_*(B_R^T)\}$; see Figures 10 and 11 (noticing that, in 10, there is a non reachable part on the top right of the figure).

After that, there are two cases to consider in order to construct (X_{k-1},Y_{k-1}).

> **Case 1:** $Y_{k-2}\le\gamma_*'(B_R^T)(X_{k-2}-B_R^T)+\gamma_*(B_R^T)$, which means that (X_{k-2},Y_{k-2}) is below the line of slope $\gamma_*'(B_R^T)$ going through $(B_R^T,\gamma_*(B_R^T))$; see Figure 12. We can pick $X_{k-1}\in(X_{k-2},B_R^T)$ and Y_{k-1} such that

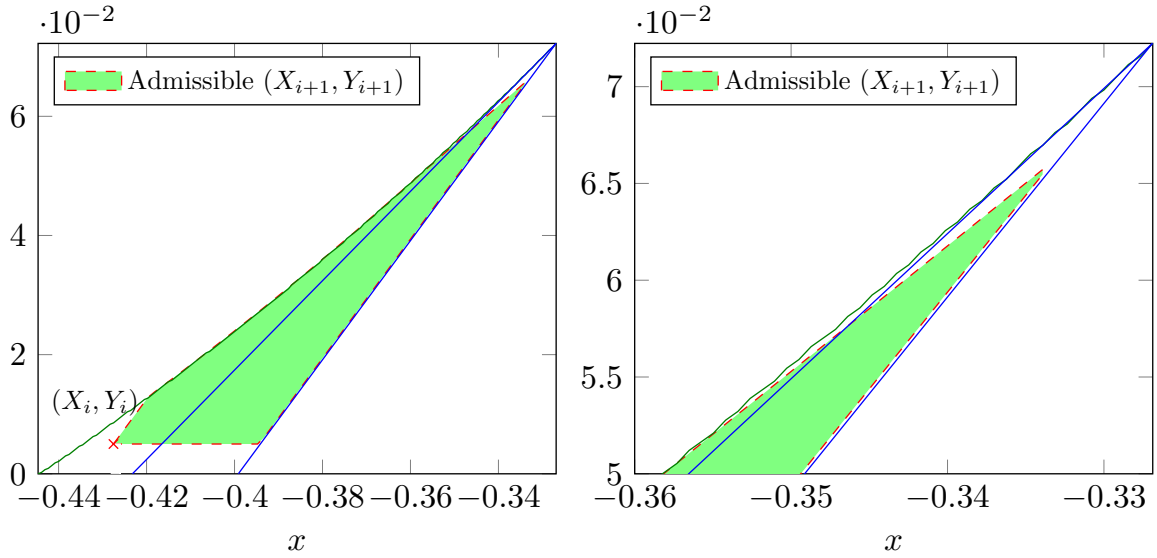

FIGURE 10. Left: Admissible choices for (X_{i+1}, Y_{i+1}) if (X_i, Y_i) is above the line of slope $\gamma_*'(B_R^T)$ going through $(B_R^T, \gamma_*(B_R^T))$. Right: Zoom for x in the interval $[-0.36, -0.33]$.

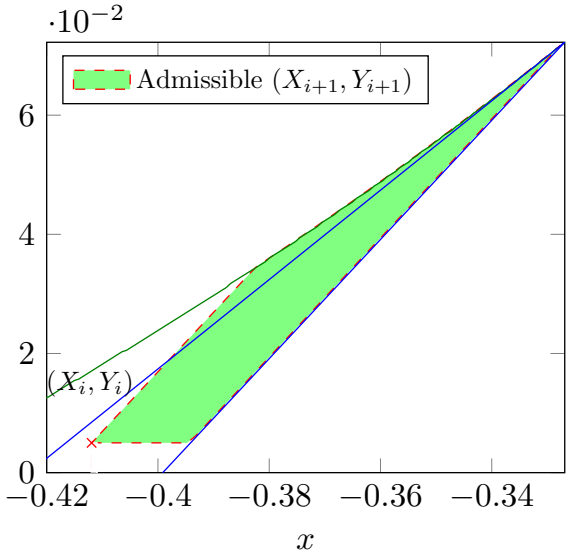

FIGURE 11. Admissible choices for (X_{i+1}, Y_{i+1}) is below the line of slope $\gamma_*'(B_R^T)$ going through $(B_R^T, \gamma_*(B_R^T))$.

(1) $Y_{k-1} \leq (X_{k-1} - B_R^T)$, which means that Y_{k-1} has to be below the line of slope $\gamma_*'(B_R^T)$ going through $(B_R^T, \gamma_*(B_R^T))$;
(2) $0 < \frac{Y_{k-1} - Y_{k-2}}{X_{k-1} - X_{k-2}} \leq 1$;
(3) $Y_{k-1} \geq \max\{Y_{k-2}, X_{k-1} - B_R^T + \gamma_*(B_R^T)\}$, which means that Y_{k-1} has to be above the line of slope 1 going through $(B_R^T, \gamma_*(B_R^T))$.

Case 2: $Y_{k-2} > \gamma_*'(B_R^T)(X_{k-2} - B_R^T) + \gamma_*(B_R^T)$, which means that (X_{k-2}, Y_{k-2}) is above the line of slope $\gamma_*'(B_R^T)$ going through $(B_R^T, \gamma_*(B_R^T))$; see Figure 13. We consider the tangent of

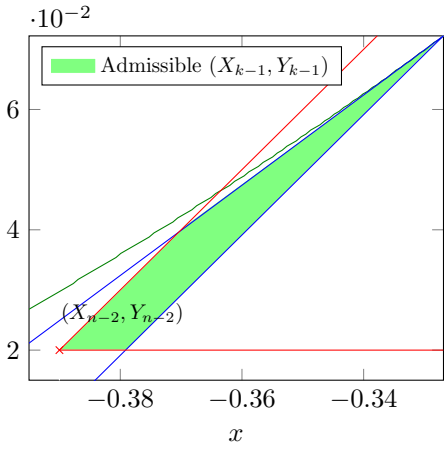

FIGURE 12. Admissible choices for (X_{k-1}, Y_{k-1}) in Case 1.

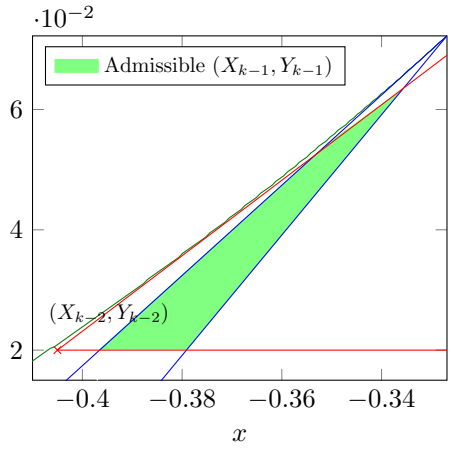

FIGURE 13. Admissible choices for (X_{k-1}, Y_{k-1}) in Case 2.

the path γ_* at a point $\underline{x} \in (X_{k-2}, B_R^T)$ going through the point (X_{k-2}, Y_{k-2}) of slope p. We can pick $X_{k-1} \in \left(\frac{Y_{k-2}-\gamma_*(B_R^T)}{\gamma_*'(B_R^T)} + B_R^T, \frac{Y_{k-2}-pX_{k-2}-B_R^T}{1-p} \right)$ and Y_{k-1} such that

(1) $Y_{k-1} \geq \max\{Y_{k-2}, X_{k-1} - (B_R^T) + \gamma_*(B_R^T)\}$;
(2) $Y_{k-1} > Y_{k-2}$;
(3) $Y_{k-1} \leq \min\{Y_{k-2} + p(X_{k-1} - X_{k-2}), \gamma_*(B_R^T) + \gamma_*'(B_R^T)(X_{k-1} - (B_R^T))\}$.

We finish the iterative construction with $(X_k, Y_k) = (B_R^T, \gamma_*(B_R^T))$.

With this new initial state $\tilde{v}_0$, we can compute a classical forward Godunov scheme to have $\tilde{v}$ in the entire domain, and we perform the backward algorithm for the transport equation with $\tilde{v}$ and w_T.

This gives us a new initial state $\tilde{w}_0$ for the transport equation and we may check that the datum $\tilde{v}_0$ and $\tilde{w}_0$ lead to a good approximation of the target (v_T, w_T); see Figure 14. To that end, we define the following *relative L^1-discrete error norms*:

$$e_v = \frac{\sum_{j=1}^{m} |v_T(x_j) - v_j^N|}{\sum_{j=1}^{m} |v_T(x_j)|}, \qquad e_w = \frac{\sum_{j=1}^{m} |w_T(x_j) - w_j^N|}{\sum_{j=1}^{m} |w_T(x_j)|}.$$

and observe that they tend to zero as Δx goes to zero; see Table 2.

Owing to Remark 5.1, we may choose the number of discontinuities that we want in D_T. For instance, considering the paths in Figure 20 yields the initial states illustrated in Figures 16, 17, 18, and 19.

ACKNOWLEDGMENTS

We thank A. Sylla, T. Liard, and E. Zuazua for several helpful conversations on topics related to this work.

Giuseppe Maria Coclite and Nicola De Nitti are members of the Gruppo Nazionale per l'Analisi Matematica, la Probabilità e le loro Applicazioni (GNAMPA) of the Istituto Nazionale di Alta Matematica (INdAM).

Giuseppe Maria Coclite has been partially supported by the Project funded under the National Recovery and Resilience Plan (NRRP), Mission 4 Component 2 Investment 1.4 -Call for tender No. 3138 of 16/12/2021 of Italian Ministry of University and Research funded by the European Union

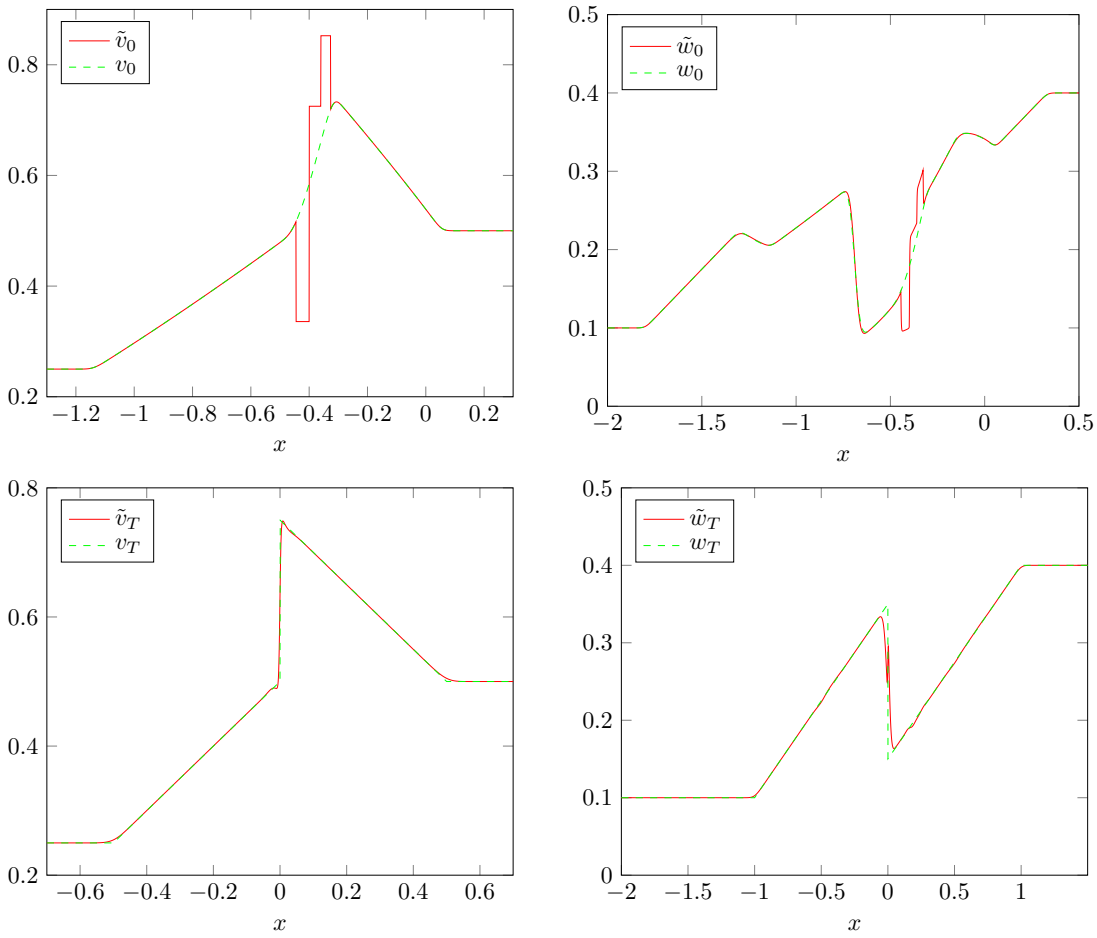

FIGURE 14. Top: initial states (v_0, w_0), obtained by backward reconstruction, and $(\tilde{v}_0, \tilde{w}_0)$, obtained by changing the initial data, leading to the target profile.
Bottom: comparison between exact profile (v_T, w_T) and recalculated target profile $(\tilde{v}_T, \tilde{w}_T)$.

-NextGenerationEUoAward Number: CN000023, Concession Decree No. 1033 of 17/06/2022 adopted by the Italian Ministry of University and Research, CUP: D93C22000410001, Centro Nazionale per la Mobilità Sostenibile and the Italian Ministry of Education, University and Research under the Programme Department of Excellence Legge 232/2016 (Grant No. CUP - D93C23000100001). GMC also expresses his gratitude to the HIAS (Hamburg Institute for Advanced Study) for their warm hospitality.

Nicola De Nitti was partially supported by the Alexander von Humboldt-Professorship program and by the Transregio 154 Project "Mathematical Modelling, Simulation and Optimization Using the Example of Gas Networks" of the Deutsche Forschungsgemeinschaft.

REFERENCES

[1] Adimurthi, S. S. Ghoshal, and G. D. V. Gowda. Optimal controllability for scalar conservation laws with convex flux. *J. Hyperbolic Differ. Equ.*, 11(3):477–491, 2014.

[2] Adimurthi, S. S. Ghoshal, and G. D. Veerappa Gowda. Exact controllability of scalar conservation laws with strict convex flux. *Math. Control Relat. Fields*, 4(4):401–449, 2014.

Δx	e_v	e_w
0.0125	0.01189	0.02914
6.25×10^{-3}	0.00673	0.02081
3.125×10^{-3}	0.00331	0.01546
1.56×10^{-3}	0.00174	0.01078
7.8×10^{-4}	0.00085	0.00735

TABLE 2. Error table of v and w.

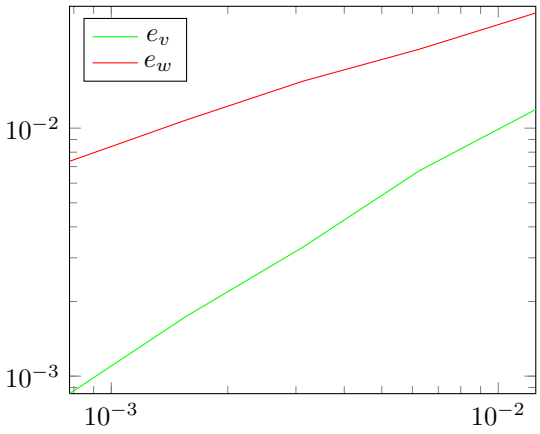

FIGURE 15. Approximation error of v and w.

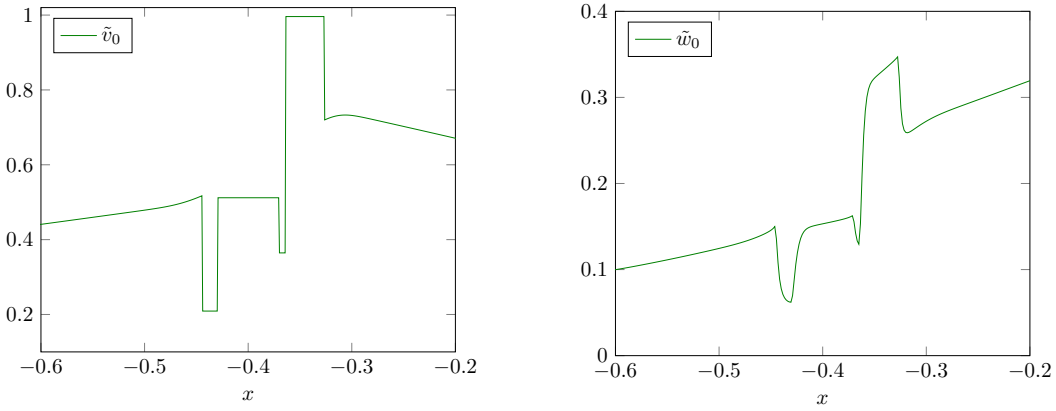

FIGURE 16. Initial state with 4 discontinuities (zoom around D_T).

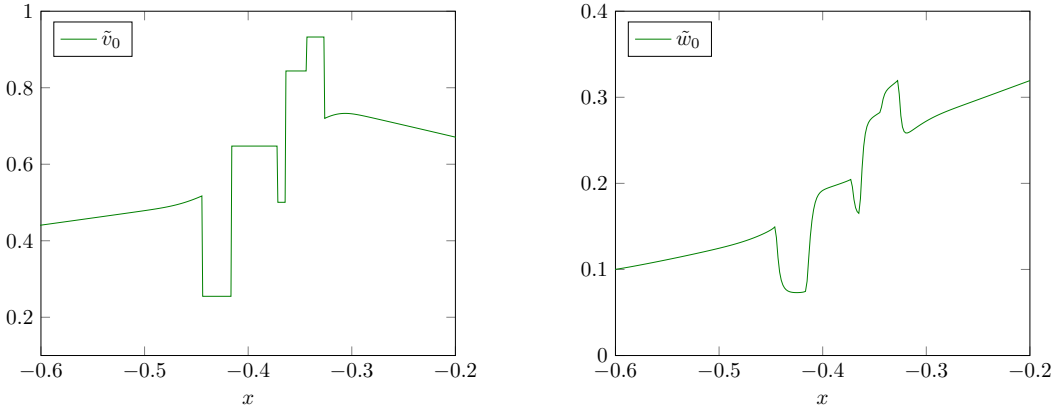

FIGURE 17. Initial state with 5 discontinuities (zoom around D_T).

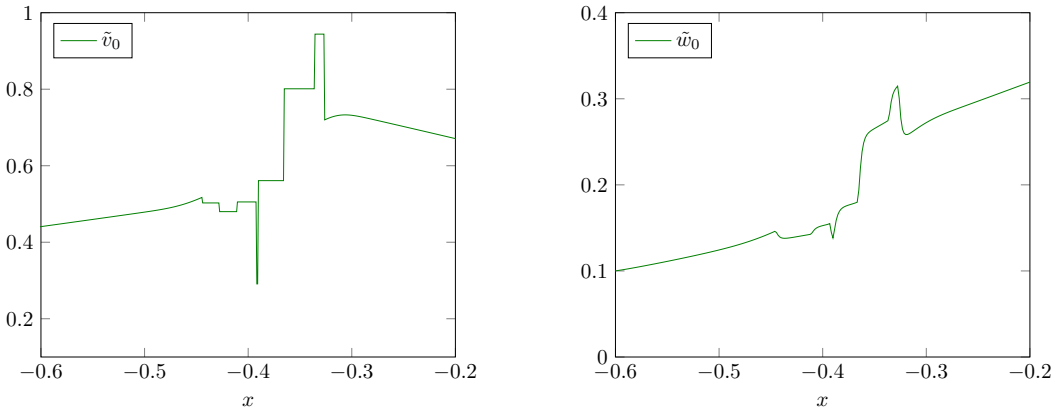

FIGURE 18. Initial state with 7 discontinuities (zoom around D_T).

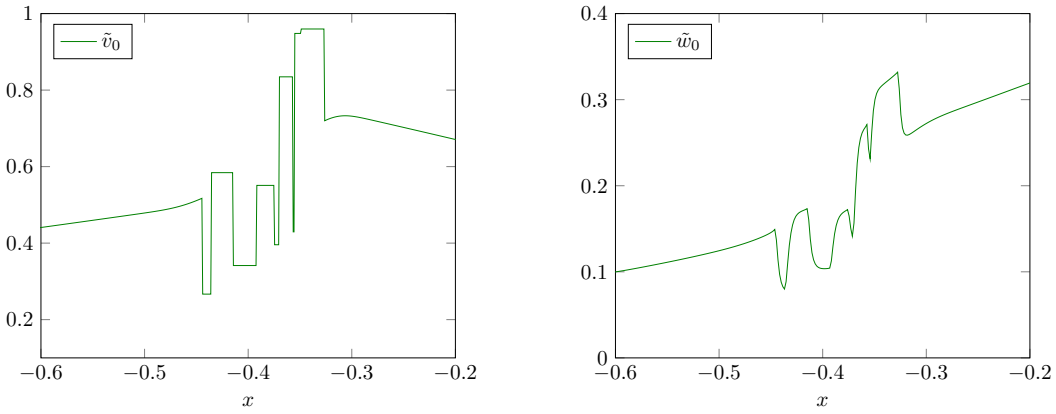

FIGURE 19. Initial state with 9 discontinuities (zoom around D_T).

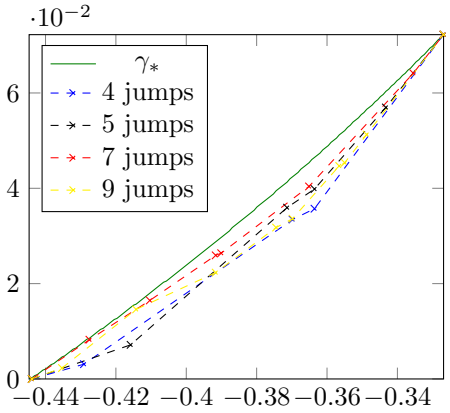

FIGURE 20. Paths for different $\tilde{v}_0$.

jumps	e_v	e_w
4	0.000727	0.00605
5	0.000715	0.00599
7	0.000777	0.00589
9	0.000715	0.00600

TABLE 3. Error table of v and w with different number of discontinuities.

[3] L. Ambrosio. Transport equation and Cauchy problem for BV vector fields. *Invent. Math.*, 158(2):227–260, 2004.
[4] L. Ambrosio, G. Crippa, A. Figalli, and L. V. Spinolo. Some new well-posedness results for continuity and transport equations, and applications to the chromatography system. *SIAM J. Math. Anal.*, 41(5):1890–1920, 2009.
[5] L. Ambrosio, G. Crippa, A. Figalli, and L. V. Spinolo. Existence and uniqueness results for the continuity equation and applications to the chromatography system. In *Nonlinear conservation laws and applications*, volume 153 of *IMA Vol. Math. Appl.*, pages 195–204. Springer, New York, 2011.
[6] L. Ambrosio, G. Crippa, and S. Maniglia. Traces and fine properties of a BD class of vector fields and applications. *Ann. Fac. Sci. Toulouse Math. (6)*, 14(4):527–561, 2005.
[7] F. Ancona and G. M. Coclite. On the attainable set for Temple class systems with boundary controls. *SIAM J. Control Optim.*, 43(6):2166–2190, 2005.
[8] F. Ancona and A. Marson. On the attainable set for scalar nonlinear conservation laws with boundary control. *SIAM J. Control Optim.*, 36(1):290–312, 1998.
[9] B. Andreianov, C. Donadello, S. S. Ghoshal, and U. Razafison. On the attainable set for a class of triangular systems of conservation laws. *J. Evol. Equ.*, 15(3):503–532, 2015.
[10] S. Bianchini. Stability of L^∞ solutions for hyperbolic systems with coinciding shocks and rarefactions. *SIAM J. Math. Anal.*, 33(4):959–981, 2001.
[11] F. Bouchut and F. James. One-dimensional transport equations with discontinuous coefficients. *Nonlinear Anal.*, 32(7):891–933, 1998.
[12] A. Bressan and P. Goatin. Stability of L^∞ solutions of Temple class systems. *Differential Integral Equations*, 13(10-12):1503–1528, 2000.
[13] A. Choudhury, G. Crippa, and L. Spinolo. Initial-boundary value problems for nearly incompressible vector fields, and applications to the keyfitz and kranzer system. *Z. Angew. Math. Phys.*, 68(138), 2017.
[14] R. M. Colombo and V. Perrollaz. Initial data identification in conservation laws and Hamilton-Jacobi equations. *J. Math. Pures Appl. (9)*, 138:1–27, 2020.
[15] R. M. Colombo, V. Perrollaz, and A. Sylla. Conservation Laws and Hamilton-Jacobi Equations with Space Inhomogeneity, 2022.
[16] R. J. DiPerna and P.-L. Lions. Ordinary differential equations, transport theory and Sobolev spaces. *Invent. Math.*, 98(3):511–547, 1989.
[17] C. Donadello and V. Perrollaz. Exact controllability to trajectories for entropy solutions to scalar conservation laws in several space dimensions. *C. R. Math. Acad. Sci. Paris*, 357(3):263–271, 2019.
[18] H. Freistühler. On the Cauchy problem for a class of hyperbolic systems of conservation laws. *J. Differential Equations*, 112(1):170–178, 1994.
[19] E. Godlewski and P.-A. Raviart. *Numerical approximation of hyperbolic systems of conservation laws*, volume 118 of *Applied Mathematical Sciences*. Springer-Verlag, New York, [2021] ©2021. Second edition [of 1410987].
[20] L. Gosse and F. James. Numerical approximations of one-dimensional linear conservation equations with discontinuous coefficients. *Math. Comput.*, 69(231):987–1015, 2000.
[21] T. Horsin. On the controllability of the Burgers equation. *ESAIM Control Optim. Calc. Var.*, 3:83–95, 1998.
[22] B. L. Keyfitz and H. C. Kranzer. A system of nonstrictly hyperbolic conservation laws arising in elasticity theory. *Arch. Rational Mech. Anal.*, 72(3):219–241, 1979/80.
[23] M. V. Korobkov and E. Y. Panov. On isentropic solutions of first-order quasilinear equations. *Mat. Sb.*, 197(5):99–124, 2006.
[24] R. J. LeVeque. *Finite volume methods for hyperbolic problems*. Cambridge Texts in Applied Mathematics. Cambridge University Press, Cambridge, 2002.
[25] T. Liard and E. Zuazua. Analysis and numerical solvability of backward-forward conservation laws. *HAL-02389808v2*, 2020.
[26] T. Liard and E. Zuazua. Initial data identification for the one-dimensional Burgers equation. *IEEE Transactions on Automatic Control*, 67(6):3098–3104, 2022.
[27] E. Panov. Generalized solutions of the Cauchy problem for a transport equation with discontinuous coefficients. In *Instability in models connected with fluid flows. II*, volume 7 of *Int. Math. Ser. (N. Y.)*, pages 23–84. Springer, New York, 2008.
[28] E. Y. Panov. On the theory of entropy solutions of the Cauchy problem for a class of nonstrictly hyperbolic systems of conservation laws. *Mat. Sb.*, 191(1):127–157, 2000.

(G. M. Coclite) Politecnico di Bari, Dipartimento di Meccanica, Matematica e Management, Via E. Orabona 4, 70125 Bari, Italy.
Email address: giuseppemaria.coclite@poliba.it

(N. De Nitti) Friedrich-Alexander-Universität Erlangen-Nürnberg, Department of Mathematics, Chair for Dynamics, Control, Machine Learning and Numerics (Alexander von Humboldt Professorship), Cauerstr. 11, 91058 Erlangen, Germany.
Email address: nicola.de.nitti@fau.de

(C. Donadello) Université de Franche-Comté, CNRS, UMR 6623, LmB, F-25000 Besançon, France.
Email address: carlotta.donadello@univ-fcomte.fr

(F. Peru) Université de Bourgogne Franche-Comté, CNRS, UMR 6623, LmB, F-25000 Besançon, France.
Email address: florian.peru@univ-fcomte.fr